Climate change accelerates recovery of the Tatra Mountain lakes from acidification and increases their nutrient and chlorophyll *a* concentrations

Jiří Kopáček*[1,2], Jiří Kaňa[1,2], Svetlana Bičárová[3], Janice Brahney[4], Tomáš Navrátil[5], Stephen A. Norton[6], Petr Porcal[1,2], Evžen Stuchlík[1]

[1]Biology Centre of the Czech Academy of Sciences, Institute of Hydrobiology, CZ-370 05 České Budějovice, Czech Republic

[2]University of South Bohemia, Faculty of Science, CZ-370 05 České Budějovice, Czech Republic

[3]Earth Science Institute, Slovak Academy of Sciences, 059 60 Tatranská Lomnica, Slovak Republic

[4]Utah State University, Department of Watershed Sciences, 5210 Old Main Hill, Logan, Utah 84322, USA

[5]Institute of Geology CAS, CZ-165 00 Prague 6, Czech Republic.

[6]Earth and Climate Sciences, University of Maine, Orono, Maine 04469, USA

*Corresponding author: Jiří Kopáček, address: Biology Centre ASCR, Institute of Hydrobiology, Na Sádkách 7, 37005 České Budějovice, Czech Republic; ORCID: 0000-0002-4409-4032; phone: +420 38 7775878; E-mail: jkopacek@hbu.cas.cz

1

Abstract

We evaluated changes in the concentration of cations, anions, nutrients (dissolved organic carbon, DOC; phosphorus, P; and nitrogen forms including nitrate, NO_3^- and total organic nitrogen, TON), and chlorophyll a (Chl-a) in 31 Tatra Mountain lakes in Slovakia and Poland during their recovery from acidic deposition (1992–2018). Typical effects of decreasing acidic deposition on the lakes' water composition, such as decreasing base cation concentrations, were confounded by climate change and catchment characteristics, including areal proportions of well-developed soils and scree. A climate-related increase in physical erosion provided freshly exposed unweathered granodiorite (the dominant bedrock) to chemical weathering. Dissolution of accessory calcite in the granodiorite increased the in-lake Ca^{2+} and HCO_3^- concentrations and reversed the Ca^{2+} trends, which originally decreased in parallel with strong acid anions. These changes were most pronounced in steep, scree-rich areas, which are most sensitive to physical weathering. Fresh apatite $[Ca_5(PO_4)_3(F,Cl,OH)]$ in the crushed granodiorite acts as a P source at soil pH's between 4 and 5 and in the presence of chelating organic acids within soils. These conditions enhance apatite solubility, which in part explains increasing P in lakes with scree-dominated catchments. Soil recovery from acidification due to decreasing acidic deposition and the neutralizing effect of weathering of erosion-derived accessory calcite were the most likely causes of elevated DOC and P export from soils. Their elevated leaching was accompanied by increasing in-lake concentrations of Chl-a and TON. The increasing TON concentrations were, as for Ca^{2+}, most pronounced in the scree-rich catchments, and represented the most sensitive indicator of the changes in the lake water nutrient composition.

Keywords: Weathering, accessory calcite and apatite, phosphorus, organic nitrogen, chlorophyll

Introduction

Ongoing changes in climate as well as the chemistry of atmospheric deposition affect the composition of waters even in seemingly undisturbed high elevation areas, significantly altering their solute concentrations and interactions between the carbon, nitrogen (N), and phosphorus (P) cycles (e.g., Camarero et al. 2009; Moser et al. 2019). Many of these freshwater ecosystems are, or have become, P-limited (Elser et al. 2009) from elevated N deposition (Wolfe et al. 20010). However, recently P concentrations have been rising in some North American (Homyak et al. 2014; Stoddard et al. 2016) and European (Camarero and Catalan 2012; Kopáček et al. 2015a) mountain waters. Several possible mechanisms for these upward P trends include climate changes and declining acidic atmospheric pollution.

Climate change alters the seasonality, amount, and intensity of precipitation, intensity of mechanical erosion, weathering, dust emissions, and the frequency of vegetation damage by insects and fires (e.g., Mast et al. 2011; Catalan et al. 2014; Brahney et al. 2015; Seidl et al. 2017). Decreasing atmospheric pollution from sulphur (S) and N compounds slows soil acidification, eventually increasing the pH of soil water. Higher pH has led to elevated leaching of dissolved organic carbon (DOC) (Driscoll et al. 2007; Monteith et al. 2007; Evans et al. 2012) and DOC-bound phosphate (Gerke 2010; Kopáček et al. 2015a). The terrestrial DOC and P co-exports are thus commonly linked (Brahney et al. 2014; Huser et al. 2018).

The most important primary P source for waters in post-glacial alpine ecosystems is release of P from apatite-rich young soils; with time, atmospheric P plays an increasing role as these ecosystems become depleted of apatite (Chadwick et al. 1999; Boyle et al. 2013). The atmospheric P flux associated with increasing dust deposition (commonly enriched with organic and apatite P compared to the ambient terrain) is a potentially important P source for alpine freshwaters in Europe and USA (Psenner 1999; Morales-Baquero et al. 2006; Brahney

et al. 2014; Stoddard et al. 2016). Globally, atmospheric deposition of P has increased compared to pre-industrial rates due primarily to increasing emissions from fossil fuels, dust, and fires (Brahney et al. 2015). In alpine areas receiving high dust inputs, lake water P concentrations are positively related to the percent of exposed bedrock in catchments and to terrain steepness (Brahney et al. 2014); these catchments have limited capacity to retain atmospherically deposited P due to sparse soil cover and short water residence time. However, few long-term trends in P deposition have been detected during the last decades (Tipping et al. 2014). Thus, elevated dust deposition may not explain recently increasing P concentrations in surface water in all alpine regions. Hence the question is, what causes increasing lake water P concentrations in watersheds that have relatively old soils, stable dust deposition, and no recent deglaciated areas in their catchments?

Kopáček et al. (2015a) suggested that increasing P concentrations in some alpine Tatra Mountain lakes (central Europe) may originate from the decreasing phosphate adsorption capacity of sparse till soils as their pH increases, because of decreasing positive charge of soil aluminium (Al) and iron (Fe) hydroxides. This mechanism may explain both increasing and decreasing trends in P leaching from soils, depending on the trajectory of soil water pH during recovery. The Tatra Mountain lakes, with increasing P availability, had high proportions of exposed bedrock and negligible proportion of meadows in their catchments, similar to the lakes with increased P in the Wind River Range, USA (Brahney et al. 2014). The Tatra Mountains are rapidly recovering from atmospheric acidification, and are affected by increasing air temperature, decreasing frequency of days with snow cover, and increasing frequency of heavy rains and freeze-thaw periods that accelerate the physical erosion of rocks (Kopáček et al. 2017). Rock fracturing is caused by ice formation and expansion in joints and microcracks in the overlying debris, and their collisions during movement due to gravity and slumping (e.g., after heavy rains) (Hall 2004; Matsuoka et al. 2008; Gislason et al. 2009). The elevated physical erosion increases the reactive surface area of rocks, supplying fresh unweathered minerals for chemical weathering. The importance of this process increases with elevation in mountain areas (Millot et al. 2002; Riebe et al. 2004). The elevated weathering is an important source of Ca^{2+} and Mg^{2+}, causing increasing trends in their concentrations in some lakes with silica-rich bedrock despite decreasing concentrations of strong acid anions (SAAs = SO_4^{2-} + NO_3^- + Cl^-) due to reduced acidic deposition (Mast et al. 2011; Rogora et al. 2013; Kopáček et al. 2017). The source of Ca^{2+} and HCO_3^- in siliceous igneous rocks is largely accessory calcite that becomes available for dissolution after physical erosion of the parent material (White et al. 2005). The freshly eroded rocks contain apatite grains that may be a source of phosphate for soil and aquatic environments (Smith et al. 1978; Welch et al. 2002; Guidry and Mackenzie 2003).

The steepest increase in Ca^{2+} concentrations in Tatra Mountain lakes occurs in the same type of lakes that have increasing nutrient concentrations, including P (Kopáček et al. 2015b; 2017). These parallel trends in Ca and P concentrations suggest that elevated weathering rates due to climate change also could contribute to the increased P leaching in some alpine catchments.

To test this potential effect of changing climate on lake water composition, we (1) evaluated long-term data on ionic chemistry and nutrient concentrations in Tatra Mountain lakes, and (2) performed laboratory weathering experiments with samples of the dominant granodiorite bedrock from the study area to estimate its potential to release Ca^{2+} and P under the ambient precipitation chemistry and soil composition. Our goal was to answer the following questions: (1) Are changes in water composition related to decreasing acidic deposition and do changes occur uniformly across catchments or are they catchment-specific? (2) Can climate change contribute to increasing lake water P concentrations in regions with

silica-rich bedrock? (3) What is a role of catchment characteristics in accelerating or modifying these processes?

Materials and methods

Site characteristics

The Tatra Mountains are situated in central Europe along the Slovak-Polish border at 20.2 °E and 49.2 °N. Bedrock is predominantly granodiorite, granite, felsic gneiss, and mica schist. Soils are dominated by humus-ferric podsol in forest areas, by shallow poorly developed podsol, leptosol, and regosol in alpine meadows (henceforth meadow soils), and by sparse poorly developed soils in scree areas (henceforth, till soils) (Kopáček et al. 2015b).

There are > 260 small, permanent and seasonal lakes of glacial origin in the Tatra Mountains; the maximum surface area is ~35 ha and maximum depth is 79 m. Most lakes are alpine, above the natural tree line, at elevations > 1800 m. The atmospheric acidification of lakes peaked in the 1980s. Since the early 1990s, the lakes have rapidly recovered from acidification due to the steep decrease in deposition of S and N (NO_3^- and NH_4^+) compounds in this region (Kopáček et al. 2015b).

For long-term monitoring, we selected 31 chemically and morphologically representative catchment-lake systems. They included a wide range in present chemistry and catchment cover, from forested (dominated by Norway spruce) to alpine (Supplementary Material, SM; Table SM-1). Most of these lakes have a maximum depth > 4 m and are thermally stratified during ice-off period. We characterized land-cover of the catchments using percentage of exposed bedrock, scree (areas of broken rocks and gravel without any vegetation except lichen), and areas covered with soil. Six lakes (henceforth, acidic lakes) had acid neutralizing capacity (ANC) < 20 µeq L^{-1} [1 eq (equivalent) is 1 mol of charge] until 2018. Acidic lakes are located in forest, dwarf pine, or alpine meadows, and have a large percentage of their catchment covered with soil (Table SM-1). Twenty-five lakes (henceforth, non-acidic lakes) either had already recovered from acidification (ANC was > 20 µeq L^{-1} in the 2010s, while < 20 µeq L^{-1} in the 1980s), or were not acidified to this threshold.

Data on soil chemistry and percentage of soil cover in catchments of lakes used in this study are from Kopáček et al. (2004, 2015a). The most important difference between the chemistry of alpine meadow and till soils was their P concentrations (25 *vs.* 35 µmol g^{-1}, respectively). Till soils had about 3-times higher concentrations of oxalate extractable soluble reactive P (SRP; 12 *vs.* 3.6 µmol g^{-1}) despite their lower phosphate adsorption capacity. For more details, see Part SM-1.

Data on daily precipitation, snow cover, and minimum, maximum, and average air temperature in the Tatra Mountains were measured at the Meteorological Observatory Skalnaté Pleso (20.234 °E, 49.189 °N, elevation of 1778 m). The data were analysed as described by Kopáček et al. (2017) for the 1965–2018 period with the following results (Fig. SM-1): Annual average air temperature significantly ($p < 0.001$) increased up to ~3–4 °C throughout 1992–2018, from their 1965–1991 average of 1.75 to 2014–2018 . The warmer 1992–2018 period had higher average annual precipitation than the 1965–1991 period (1.46 *vs.* 1.30 m yr^{-1}). Annual number of days with snow cover (> 2 cm) significantly decreased ($p < 0.001$), while numbers of days yr^{-1} without precipitation ($p < 0.05$) and with high precipitation amount (>30 mm day^{-1}, $p < 0.01$) significantly increased during 1992–2018. Frequency of days with air temperature fluctuating through the freezing point (daily minimum < 0 °C and daily maximum > 5 °C) continuously increased ($p < 0.001$) during 1992–2018.

Data on chemical composition of bulk precipitation in the study area (Kopáček et al. 2015b and Mitošinková M. *pers. commun.*) are from the Chopok meteorological station, situated in the Low Tatra Mountains at 19.590 °E, 48.944 °N and elevation of 2008 m.

Data on the bulk P deposition in the Tatra Mountains are from Kopáček et al. (2011). Volume-weighted mean concentration of total phosphorus (TP) and SRP in bulk precipitation averaged 0.59 and 0.30 μmol L^{-1}; the average bulk deposition of TP was 0.7 mmol m^{-2} yr^{-1}.

Water sampling and analyses
Lake water was collected once annually in September to early October before ice-on and analysed for ANC (Gran titration), major ions, reactive silica (Si), dissolved organic carbon (DOC), TP, total organic nitrogen (TON), and chlorophyll *a* (Chl-*a*). Details on sampling and analyses are in Kopáček et al. (2015b, 2017) and Table SM-2. Positive ANC values were assumed to represent HCO_3^- concentrations and $HCO_3^- = 0$ was used for all ANC values ≤ 0 μmol L^{-1}. We neglected any effect of organic acid anions on ANC in this estimate because changes in their charge during sample titration from an ambient pH to ~4.5 (an approximate pH value where all HCO_3^- is titrated to the dissolved CO_2) were < 3 μeq L^{-1}.
The average solute concentrations in the 6 acidic and 25 non-acidic lakes were computed as the average annual mean for all lakes in each category. The number of annual observations ranged from 15–27 for individual lakes. Linear regressions of concentrations of water solutes against time were used to determine slopes and significance of trends in lake water composition (Ca^{2+}, Mg^{2+}, H^+, SO_4^{2-}, NO_3^-, Cl^-, ANC, TP, Chl-*a*, TON, DOC, and Si) in each lake over the 1992–2018 period. Percentage changes in concentrations of TP, Chl-*a*, DOC, and TON (Δ; % yr^{-1}) were calculated as 100×(slope/average) during the 1992–2018 period. We also used the Mann-Kendall test (R Development Core Team 2015) to confirm significance of long-term trends in water chemistry, because some data did not meet the assumption of normality.

Bedrock sampling, analyses, and extraction experiments
Bedrock chemical analyses were performed following Kopáček et al. (2017). Twelve representative unweathered samples of the dominant granodiorite bedrock (G1 to G12) were collected from scree areas in four catchments (Table SM-1). All samples were crushed and analysed for basic chemical and mineralogical compositions, and apatite composition (Tables SM-3 to SM-5). We used the 2–5 mm size fraction of crushed samples for extraction experiments.
Prepared samples (16 g) were extracted 24 hours at 20–25 °C with 80 ml of 0.32 mmol HNO_3 L^{-1}. Initial pH of extraction solution was 3.5 for all samples and 5.0 (0.01 mmol HNO_3 L^{-1}) for seven samples (three samples with the highest and four samples with the lowest carbonate content). We averaged results from three replicates for data evaluation. The extraction was repeated 15 times with new solution. After filtration of extraction solutions, concentrations of base cations (BCs = Ca + Mg + Na + K), Al, Fe, and Si were determined using inductively coupled plasma mass spectrometry (8800 Triple Quadrupole ICP-MS analyser), concentration of P was measured as SRP following Murphy and Riley (1962), HCO_3^- production was estimated as positive ANC, and H^+ consumption was computed as the difference from H^+ concentrations at the beginning and end of each extraction step. The average pH of extraction solution for the 15 consecutive extractions was calculated from average H^+ concentration at the end of each step. Total amounts of elements, HCO_3^-, and SRP dissolved from rocks (and consumed H^+) during the 15 extractions was computed as the sum of all steps. All released SRP was assumed to originate from apatite. The amount of Ca originating from apatite dissolution (Ca-apatite) was estimated from production of SRP multiplied by the Ca:P ratio in apatite (1.51–1.68) in individual samples. The difference between the total released Ca and apatite-Ca was assumed to originate from dissolution of accessory calcite in rocks (calcite-Ca), recognizing that small contributions would be from

weathering of Ca-bearing silicates. Details on experimental design and rock composition, including their carbonate content, are in Part SM-2.

The apatite standard (A1) was from the Institute of Geology, Czech Academy of Science. We used 2–5 mm fractions of the crushed sample A1 and tested the effect of pH on the release of Ca and P during a 24-hour extraction with 0.32 mmol HNO_3 L^{-1} (pH = 3.5), and oxalic and citric acids (both 1 mmol L^{-1}). All acidic solutions were titrated with NaOH to obtain starting pH values of extraction solutions in the range from 3.5 to ~7 (for more experimental details, see Part SM-2).

Results
Water chemistry
Chemistry of the 31 selected Tatra Mountain lakes varied widely. The 1992–2018 average concentrations of SAAs, HCO_3^-, and Ca^{2+} + Mg^{2+} (representing 85% of BCs) were 42–120, 0–313, and 28–413 µeq L^{-1}, respectively (Table SM-6). Water chemistry has been rapidly recovering from atmospheric acidification, with continuously decreasing SAA concentrations and increasing HCO_3^- and pH in both acidic and non-acidic lakes since 1992 (Fig. 1; for trends in concentrations of major solutes see Tables SM-7 and SM-8). Between the 1992–1995 and 2015–2018 periods, the respective average (± standard deviation) water composition of the non-acidic and acidic lakes changed as follows: concentrations of SAAs decreased from 106±23 to 52±14 and from 93±18 to 33±13 µeq L^{-1}; ANC increased from 86±72 to 141±82 and from −12±7 to 10±7 µeq L^{-1}; and pH increased from 6.1±0.5 to 6.8±0.3 and from 4.8±0.1 to 5.4±0.3. In acidic lakes, the decrease in SAA concentrations was partly compensated for by decreasing concentrations of Ca^{2+} + Mg^{2+} throughout the study. In non-acidic lakes, the Ca^{2+} + Mg^{2+} concentrations decreased together with SAAs to the middle 2000s, then the Ca^{2+} + Mg^{2+} concentrations started to increase (Fig. 1b), despite a continuing decrease in SAAs (Fig. 1a).

Concentrations of all major ions in bulk precipitation [SO_4^{2-}, NO_3^-, NH_4^+, H^+, and (Ca^{2+} + Mg^{2+})] have been decreasing in the study area since the 1990s (Fig. SM-2).

Average concentrations of DOC and TON increased significantly (p <0.001) in both lake categories, while the average TP concentrations slightly increased (p <0.05) only in acidic lakes (Fig. 2). Despite the absence of general increase in TP averages for the 25 non-acidic lakes, significant increases occurred in four of them. Significant increases in Chl-*a* concentrations occurred in seven non-acidic lakes, and the type average for this category significantly (p <0.05) increased from 1992–2018 (Fig. 2b). Concentrations of Si exhibited no consistent trends (Table SM-7).

Slopes of changes in concentrations of major water constituents were highest in lakes with high 2018 concentrations, and related to catchment characteristics. During 1992–2018, concentrations of SO_4^{2-} decreased more steeply in lakes with high percentage of soil area in the catchment area (soil-rich catchments) (Fig. 3a), while NO_3^- concentrations decreased more steeply in soil-poor catchments (Fig. 3b); concentrations of DOC increased more steeply in soil-rich catchments (Fig. 3c); and the ANC increase was steepest in soil-poor catchments (Fig. 3d).

Relative changes in concentrations of TP ranged between −1.5 and 2.2 % yr^{-1} during 1992–2018 and positively correlated with scree area in the lake catchments (Fig. 4a). Similar positive correlations between scree cover and relative concentration changes also occurred for ΔChl-*a*, ΔTON, and ΔDOC, with the respective ranges of −2 to 10, 1 to 4, and 0.3 to 6 % yr^{-1} (Fig. 4). The most pronounced relative changes in concentration of nutrients and Chl-*a* thus occurred in lakes with high scree proportions in their catchments. In contrast, we observed no relationships between these variables and the percentage of either soil area or exposed rocks in the catchments (not shown).

Leaching experiments with granodiorite
Major mineral components of the granodiorite were plagioclase (35%), quartz (30%),
muscovite (14%), and K-feldspar (11%). Calcite and apatite were present in trace amounts.
Chemical composition of granodiorite samples was dominated by Si and Al (12 and 3 mmol
g^{-1} on average, respectively); Na, K, Ca, and Mg averaged 1.3, 0.6, 0.4, and 0.2 mmol g^{-1},
respectively. Carbonate and P concentrations ranged from < 2–89 and 7–19 µmol g^{-1},
respectively. Chemical composition of apatite was similar in all 12 granodiorite samples, with
the average Ca:P:O:F atomic ratio of 4.9:3.0:12.6:1.0. This ratio was similar to that of the
apatite used in further experiments (see below).

   The amounts of BCs dissolved from samples during the first 15 extraction steps with 0.32
mM HNO_3 (original pH = 3.5) ranged from 2–30 µeq g^{-1}. The extracted BCs were dominated
by Ca, representing 83±13% of the total BC sum, while K, Na, and Mg contributed 7±6, 6±6,
and 4±3%, respectively. The amount of extracted calcite-Ca was positively correlated ($p <$
0.001) with the concentration of bicarbonate, while a negative correlation ($p < 0.05$) occurred
between apatite-Ca and bicarbonate (Fig. 5a). The reason for this negative correlation was the
positive effect of carbonate concentration on the final pH of the extraction solution and
negative effect of higher pH on apatite solubility.

   In samples G2 and G6, consumption of H^+ was higher than their carbonate content,
suggesting a partial dissolution of other minerals, mostly apatite. In contrast, the 15 extraction
steps only dissolved 18% and 22% of total carbonate from samples G1 and G11 that had the
highest carbonate concentration, as calcite (Table SM-3). The 15 extraction steps dissolved
52±20% of the carbonate in the rest of granodiorite samples (excluding G1, G2, G6, and
G11).

   The amount of SRP extracted in the 15 extraction steps ranged from 0.08–1.3 µmol g^{-1},
representing < 8% of total P in the samples. The amount of extracted SRP significantly ($p <$
0.01) increased with the decreasing final pH of extraction solution (Fig. 5b). Less than 1% of
total P in samples was released as SRP from carbonate-rich samples where the average final
pH was not < 5 during the 15 extraction steps. In contrast, in samples with lower carbonate
content, the average final pH was from 3.6–4.9, and the total leached SRP represented 4–8%
of the total P in rocks (Table 1). Because the pH of extraction solution was controlled mostly
by the concentration of carbonate in samples, more SRP and apatite-Ca were dissolved from
samples with low carbonate content and negative correlation ($p < 0.001$) occurred between
dissolved HCO_3^- and SRP concentrations given in Table 1.

   This experiment showed that all samples of unweathered granodiorite were important
sources of Ca and SRP ions and 50% of them also of HCO_3^- (Table 1). The accessory calcite
was the major source of Ca and HCO_3^-, while apatite was the most likely source of SRP. The
15 extraction steps yielded a relatively small fraction of the total available calcite and apatite.
This was likely caused by the coarse grain size (2–5 mm) used in the experimental
weathering, with calcite and apatite occluded within other crystals, or just partially dissolved
because of the short exposure time. Rock fragments only became a significant source of SRP
at pH < 5. This lower limit was confirmed by the experiment using 0.01 mM HNO_3 solution
(initial pH = 5). The final average pH of extraction solutions in the 15 consecutive steps
ranged from 5.2 to 8.8, concentrations of dissolved Ca^{2+} were equal to the amount of
dissolved carbonate (measured as HCO_3^- and neutralized H^+), and SRP concentrations were
negligible (Fig. SM-3).

Leaching experiments with apatite
The chemical composition of apatite A1 was similar to the trace apatite in the granodiorite
samples, with the Ca:P:O:F atomic ratio of 5.2:3.1:13.2:1.0. The amount of SRP dissolved

during the 24-hour extraction was negligible at pH > 6, but then exponentially increased with decreasing pH to 3.5 for all acids (Fig. 6). The efficiency of individual acids to dissolve apatite from initially the same pH increased in the order HNO_3 < citrate << oxalate (Fig. 6), indicating that organic acids were more effective solvents than HNO_3 at the same pH.

Discussion

Major ions

The 1992–2018 time series of ionic concentrations in the Tatra Mountain lakes predominantly reflected decreasing atmospheric deposition of S and N compounds, but the steepness of their changes was further modified by catchment characteristics, in-lake processes, and climate change effects on lake catchments as follows:

(1) Decreases in lake water SO_4^{2-} concentrations were steeper in soil-rich catchments (i.e., in areas covered with vegetation) than in scree and bare rock areas (Fig. 3a) due to higher SO_4^{2-} inputs to forest foliage than to bare surface (Křeček et al. 2019). Reduction in concentrations of sulphur compounds in the atmosphere resulted in a steeper decrease in SO_4^{2-} concentrations in throughfall than in bulk deposition (Oulehle et al. 2016).

(2) The extents of catchment saturation with N, as well as NO_3^- losses to waters were higher in soil-poor than in soil-rich catchments (Kopáček et al. 2005). The decrease in N deposition thus caused more pronounced reduction in NO_3^- leaching from soil-poor than soil-rich catchments (Fig. 3b). Similar relationships between NO_3^- concentrations in surface waters and soil pools or vegetation density in their catchments (i.e., catchment pools of organic carbon) are commonly reported from other mountain areas (Baron et al. 2000; Goodale et al. 2000; Evans et al. 2006; Camarero et al. 2009).

(3) The lake water concentrations of NO_3^- and SO_4^{2-} were lower than the terrestrial export owing to in-lake microbial reduction, pointing to a strong internal acid neutralizing (ANC generating) process (Cook et al. 1986; Kelly et al. 1987). The fraction of external NO_3^- loading that was reduced in the Tatra Mountain lakes [calculated from water residence time according to Kelly et al. (1986)] was 6–64%, with an average of 25% (Kopáček et al. 2005). Similarly computed in-lake SO_4^{2-} reduction was 0.4–11%, with an average of 3%. These processes are first order reactions and their rates increase with increasing concentrations of reactants (Kelly et al. 1987). Consequently, they contributed more to the in-lake NO_3^- and SO_4^{2-} reduction and ANC production in the 1990s than in the 2010s, and cannot explain the observed increase in HCO_3^- concentrations (Fig. 1c).

(4) Lakes in soil-rich catchments (Table SM-1) had high DOC and low ANC concentrations (Table SM-6). Reduced acidic deposition resulted in elevated DOC leaching from numerous recovering areas (Monteith et al. 2007; Evans et al. 2012). The steepest DOC increase reflected the steepest decrease in SO_4^{2-} concentrations in the soil-rich Tatra Mountain catchments (Figs. 3a,c), consistent with other areas. The elevated leaching of DOC, including organic acids, restricted ANC recovery in the soil-rich catchments more than in soil-poor catchments and delayed their recovery from acidification. Moreover, the steeper ANC increases in lakes in soil-poor (scree-rich) areas also benefited from a higher rate of physical rock erosion and HCO_3^- production from accessory calcite in these catchments since the middle 2000s (Kopáček et al. 2017). The increasing DOC leaching from soil-rich catchments and elevated rock weathering in the scree-rich catchments were thus responsible for a negative relationship between the rate of ANC change in the lakes and percent soil cover in their catchments (Fig. 3d)

(5) Concentrations of BCs (dominated by Ca^{2+}) decreased concurrently with concentrations of SAAs in all lakes. This decline continued in the acidic lakes until 2018, while in the non-acidic lakes only to the middle 2000s. Then, the decreasing trends in $Ca^{2+} + Mg^{2+}$ concentrations reversed and started to increase, together with HCO_3^-, in the non-acidic lakes

(Fig. 1b,c). This change cannot be explained by elevated dust deposition, as in some North American western mountain lakes (Brahney et al. 2013) due to continuously decreasing concentrations of $Ca^{2+} + Mg^{2+}$ in bulk precipitation in the Tatra region, including wet and dry vertical deposition (Fig. SM-2). Moreover, the absence of glaciers and rock glaciers excludes the possibility of increasing solute release during melting in the Tatra Mountains as compared with the Alps (Thies et al. 2007; 2013). And finally, the recently increasing trends in $Ca^{2+} + Mg^{2+}$ concentrations cannot be explained by the in-lake process associated with BC desorption for H^+ in sediments that occurs during acidification (Schiff and Anderson 1986; Norton et al. 1990). During recovery from acidification, the process would reverse, decreasing lake water BCs. Thus, the increasing trends of Ca^{2+} in the Tatra Mountain lakes, similarly to HCO_3^- concentrations, were probably caused by elevated physical erosion of granodiorite rocks and dissolution of freshly exposed accessory calcite (Kopáček et al. 2017). Laboratory experiments showed that Ca^{2+} and HCO_3^- ions dissolve from the crushed granodiorite in a wide pH range (Figs. 5 and SM-3). Precipitation thus can efficiently dissolve Ca^{2+} and HCO_3^- from the accessory calcite exposed by physical erosion of rocks and increase their concentrations in lakes, even as the pH of atmospheric deposition increases. This process is more effective in scree areas with higher proportion of exposed rocks and steeper slopes where rocks are not thermally insulated and stabilized by soils (Kopáček et al. 2017). The BCs *vs.* SAAs trends thus decoupled in the non-acidic lakes with large scree areas in the middle 2000s, while they exhibited parallel trajectories in the acidic, soil-rich, catchments during the whole study (Fig. 1b).

Nutrients
Concentrations of TON significantly increased in most acidic and non-acidic lakes in the Tatra Mountains from 1992–2018 (Fig. 2d, Table SM-7). Besides elevated terrestrial export of TON (together with DOC), this increase probably reflected elevated P availability (decreasing P limitation of phytoplankton and thus higher primary production) in these lakes (Kopáček et al. 2015a). Concentrations of TP and Chl-*a* increased in most lakes from 1992–2018; however, in contrast to DOC and TON, slopes of their increases were significant only in a few lakes (Table SM-7). The lower significance in the TP trends may be caused by their low concentrations, close to the detection limit (Table SM-2) in non-acidic lakes. The TON concentrations thus appear to be the most sensitive indicator of changes in the lake water nutrient concentrations.

Concentrations of DOC, TON, TP, and Chl-*a* in the Tatra Mountain lakes increased along a gradient of increasing percentage of soil and vegetation cover in their catchments (Kopáček et al. 2015a). The percent changes in their concentrations, however, significantly increased with percentage of scree in catchments (Fig. 4). Such a pattern in the lake nutrient concentrations could be potentially explained by the increasing dust deposition, as observed elsewhere (e.g., Morales-Baquero et al. 2006; Camarero and Catalan 2012; Tsugeki et al. 2012), because scree-rich catchments have low capacity to retain atmospherically deposited P (Brahney et al. 2014). However, we did not observe increasing TP deposition in the Tatra Mountains or at regionally close research plots in the Czech Republic (Kopáček et al. 2011). Elevated dust inputs would also be a source of Ca^{2+} (Vicars and Sickman 2011; Brahney et al. 2013), the concentration of which is decreasing in precipitation. An increase in atmospheric P input is thus an unlikely reason for the increasing TP, TON, and Chl-*a* concentrations in the Tatra Mountain lakes.

Positive relationships between lake water DOC and TP concentrations (Kopáček et al. 2015b; Fig. 4) may be associated with their linked export from soils. As soil water pH increases above 3.5–4, positive charge of Al and Fe hydroxides in soils decreases, decreasing their capacity to bind anions, including organic acids and phosphate (Kaňa et al. 2011;

Kopáček et al. 2015a). Moreover, organic acid anions compete with phosphate for binding sites in soils (Patrick and Khalid 1974). The increasing DOC concentrations in soil water during recovery from acidification (Evans et al. 2012) can increase phosphate desorption (or decrease adsorption of atmospherically deposited phosphate) and formation of soluble DOC-Fe(Al)-phosphate complexes (Gerke 2010), increasing P mobility and in-lake TP concentrations. In concordance with this mechanism, the increases in concentrations of DOC and TP were steeper in the acidic lakes (with soil-rich catchments) than in non-acidic lakes (Fig. 2). In contrast, the relative changes in lake water TP concentrations were steeper in catchments with more abundant scree areas (Fig. 4). Some of these presently non-acidified lakes in scree-rich catchments were acidified in the 1980s and exhibited steep recovery trends (Stuchlík et al. 2017). Changes in their chemistry are consistent with a conceptual model by Gerson et al. (2016) that predicts a decrease in P limitation in freshwater ecosystems after decreased atmospheric N and S deposition due to increasing terrestrial P leaching associated with decreasing P adsorbing capacity of soils and elevated P co-export with DOC.

The scree areas are dominated by till soils. The average concentrations of total P are 40% higher in the till than alpine meadow soils despite their lower concentrations of Al and Fe hydroxides (Kopáček et al. 2004). The lower concentrations of Al and Fe hydroxides (the dominant phosphate-binding phases) in the till soils cause their higher ability (compared to alpine meadow soils) to desorb phosphate at increasing pH (Kopáček et al. 2015a). Catchments with lower proportions of till than alpine meadow soils have lower overall DOC and P leaching and lower in-lake concentrations, but the higher sensitivity of till soils to pH increase causes higher relative changes of DOC and P leaching in the scree-rich catchments. The amount of phosphate that can be desorbed from soils depends on soil adsorption capacity given by concentrations and age of Al and Fe hydroxides and soil water pH (Detenbeck and Brezonik 1991; Kaňa et al. 2011) and the amount of adsorbed phosphate. Now, a question arises: "Why are TP concentrations higher in the till than alpine meadow soils?" We discuss possible answers in the next section.

Phosphorus sources and pools
Lake water TP concentrations (0.05–0.47, average of 0.13 μmol L^{-1}) were lower than in bulk precipitation (0.59 μmol L^{-1}). Some of this P was retained in the lake sediments. The fraction of external TP loading buried in sediments (calculated from water residence time) varied within 13–65%, with an average of 34% (Kopáček et al. 2011). This in-lake phosphorus retention does not explain all the difference between precipitation and lake water TP concentrations, strongly implying that only a fraction of the TP deposited to catchments enters the lakes. The TP concentrations in both alpine meadow and till soils are about two times higher than in bedrock (14 μmol g^{-1} on average; Table SM-3). The TP pools averaged 2.93 mol m^{-2} in the Tatra Mountain meadow soils from their surface to bedrock (Kopáček et al. 2004). If all mineral material in the fine meadow soil (determined from the ash content and average P concentration in bedrock) were unweathered bedrock fragments, the average TP pools should be 1.44 mol m^{-2}. The meadow soils were thus enriched by 1.49 (2.93 – 1.44) mol m^{-2} TP. This difference would be reached after ~2,040 years at the current rate of atmospheric TP deposition of 0.7 mmol m^{-2} yr^{-1}, provided all atmospherically deposited TP was retained in soils. We cannot estimate TP pools associated with till soil in scree areas because they were only sampled to the shallow subsurface. We found, on average, 13 kg till soil m^{-2} just below the surface stones (sampled to the maximum depth of < 0.8 m; Kopáček et al. 2004), but it is highly probable that other buried soils exist deeper in the scree. If the total mass of till soil per area is lower than in alpine meadows, their higher TP concentrations could simply originate from accumulation of atmospherically deposited TP in lower mass of soil. Another potential P source for till soil is, however, the elevated apatite availability from

physical weathering that is higher in the steep scree terrain than in alpine meadows (Kopáček et al. 2017).

Similarly to previous studies (e.g., Guidry and Mackenzie 2003), our laboratory extraction experiments showed that the physically eroded granodiorite could be a source of SRP and Ca^{2+} at pH < 5 (Fig. 5). The present pH of bulk precipitation is ~5 (Fig. SM-2) and is too high to effectively dissolve apatite in the samples. Thus, the granodiorite particles directly exposed to precipitation probably are not a significant P source for lakes. However, if these particles enter the till soils, they could become a P source for the soil microbial community. Several culture experiments (e.g., Smith et al. 1978; Wallander et al. 1997; Welch et al. 2002) have demonstrated that bacteria, fungi, and algae can solubilize apatite at circum-neutral pH and this process is more effective as particle size decreases. This indicates that the freshly crushed granodiorite particles with exposed apatite grains have the potential to be a source of phosphate for soil microbial community. Microorganisms produce organic acids (such as pyruvate, fermentation products, and oxalate) and CO_2, all of which lower soil water pH, and increase apatite dissolution by up to an order of magnitude compared to the inorganic conditions, due to chelating effects of some (e.g., oxalic) acids (Welch et al. 2002). Consistent with studies by Boyle et al. (2013) and Welch et al. (2002), we observed increased apatite solubility with HNO_3 at the ambient soil pH (4–5), and increased solubility in the presence of oxalic acid (Fig. 6). In addition, P uptake from apatite can be supported by soil fungi due to high affinity of their mycelia for dissolved P (Wallander et al. 1997; Blum et al. 2002). Phosphate liberated from dead microbial biomass is then adsorbed on Al and Fe hydroxides, thereby increasing the soil TP concentrations.

We suggest that present climate-change has elevated physical erosion, providing freshly exposed unweathered granodiorite containing apatite for till soil. The elevated availability of apatite for soil microbial community can support their growth, transforming P from the inorganic, poorly soluble form, to organically-bound P, and finally to phosphate bound on the soil adsorption complex. The extra apatite in scree areas compared to alpine meadows thus may explain the three-times higher concentrations of mineral P forms in the till soils despite their lower phosphate adsorption capacity. As soil water pH increases in till soils due to their recovery from acidification, adsorbed phosphate may desorb and leach to lakes (Kopáček et al. 2015a).

The negative relationship between the release of Ca from calcite and Ca from apatite (Fig. 5a) suggests that the transformation of apatite P to phosphate adsorbed on soils can be retarded by the presence of accessory calcite. Soil water acidity is neutralized by calcite dissolution, while efficient apatite dissolution begins only after calcite depletion. The freshly crushed granodiorite rocks thus may become a P source after a substantial delay. The dissolution of accessory calcite can, however, rapidly increase soil water pH and desorb already bound phosphate from Al and Fe hydroxides or, alternatively, decrease the extent of adsorption of atmospherically deposited phosphate on the soil sorption complex. The elevated inputs of accessory calcite from physical weathering to the till soils thus could have this indirect effect on elevated P leaching and increasing TON and Chl-*a* concentrations of lakes with scree-rich catchments.

Conclusions

Changes in major ion and nutrient concentrations in the Tatra Mountain lakes are an interplay between their recovery from acidic deposition and a changing climate. Proportions of meadow soils and scree areas in catchments influence the impacts of atmospheric pollution and climate on lake water chemistry. Consequently, the effects of S and N deposition and climate change on lake water composition are not uniform and result in different trends in concentrations of lake water solutes. Decreasing acidic deposition uniformly results in decreasing

concentrations of SAAs in all types of lakes. Their decline is initially accompanied by decreasing concentrations of Ca^{2+} and Mg^{2+} in acidic lakes in soil-rich catchments, but climate change reversed this trend in non-acidic lakes in scree-rich areas due to elevated dissolution of Ca^{2+} and HCO_3^- from accessory calcite (Fig. 1). This latter process is most pronounced in steep catchments where the scree is less stable and more exposed to physical erosion and weathering than rocks and gravel insulated by soils.

The elevated physical erosion of granodiorite and exposure of unweathered apatite grains to soil water is a potential source of P in the scree-rich catchments. The direct effect of climate change on TP concentrations in the Tatra Mountain lakes is not substantial at the present pH of bulk precipitation. However, apatite in lower pH and higher organic acid environments of till soil can dissolve, increasing P bound in the soil sorption complex.

The highest increase in lake water DOC, TON, and TP concentrations during recovery from acidification occurred in acidic, soil-rich catchments (Fig. 2, Table SM-1). In contrast, the most pronounced relative change in lake water concentrations of DOC, TP, TON and Chl-*a* occurred in lakes with scree-rich areas (Fig. 4). We hypothesize that soil recovery from acidification and dissolution of accessory calcite from physical erosion increase soil water pH and decrease soil's capacity to bind organic acid anions and phosphate, causing their elevated leaching and the observed increasing lake water concentrations of nutrients.

References
Baron JS, Rueth HM, Wolfe AM, Nydick KR, Allstott EJ, Minear JT, Moraska B (2000) Ecosystem responses to nitrogen deposition in the Colorado Front Range. Ecosystems 3:352–368

Blum JD, Klaue A, Nezat CA, Driscoll CT, Johnson CE, Siccama TG, Eagar C, Fahey TJ, Likens GE (2002) Mycorrhizal weathering of apatite as an important calcium source in base-poor forest ecosystems. Nature 417:729–731

Boyle JF, Chiverrell RC, Norton SA, Plater AJ (2013) A leaky model of long-term soil phosphorus dynamics. Global Biogeochem Cy 27:516–525

Brahney J, Ballantyne AP, Sievers C, Neff JC (2013) Increasing Ca^{2+} deposition in the western US: The role of mineral aerosols. Aeolian Res 10:77–87

Brahney J, Ballantyne AP, Kociolek P, Spaulding S, Out M, Porwoll T, Neff JC (2014) Dust mediated transfer of phosphorus to alpine lake ecosystems of the Wind River Range, Wyoming, USA. Biogeochemistry 120:259–278

Brahney J, Mahowald N, Ward DS, Ballantyne AP, Neff JC (2015) Is atmospheric phosphorus pollution altering global alpine lake stoichiometry? Global Biogeochem Cy 29(9):1369−1383

Camarero L, Rogora M, Mosello R, Anderson NJ, Barbieri A, Botev I, Kernan M, Kopáček J, Korhola A, Lotter AF, Muri G, Postolache C, Stuchlík E, Thies H, Wright RF (2009) Regionalisation of chemical variability in European mountain lakes. Freshwater Biol 54: 2452–2469

Camarero L, Catalan J (2012) Atmospheric phosphorus deposition may cause lakes to revert from phosphorus limitation back to nitrogen limitation. Nat Commun 3:118

Catalan J, Pla-Rabés S, García J, Camarero L (2014) Air temperature-driven CO_2 consumption by rock weathering at short timescales: Evidence from a Holocene lake sediment record. Geochim Cosmochim Ac 136:67–79

Chadwick OA, Derry LA, Vitousek PM, Huebert BJ, Hedin LO (1999) Changing sources of nutrients during four million years of ecosystem development. Nature 397:491–497

Cook RB, Kelly CA, Schindler DW, Turner MA (1986) Mechanisms of hydrogen ion neutralization in an experimentally acidified lake. Limnol Oceanogr 31:134–148

Detenbeck NE, Brezonik PL (1991) Phosphorus sorption by sediments from a soft-water seepage lake. 2. Effects of pH and sediment composition. Environ Sci Technol 25:403–409

Driscoll CT, Driscoll KM, Roy KM, Dukett J (2007) Changes in the chemistry of lakes in the Adirondack region of New York following declines in acidic deposition. Appl Geochem 22:1181–1188

Elser JJ, Andersen T, Baron JS, Bergström AK, Jansson M, Kyle M, Nydick KR, Steger L, Hessen DO (2009) Shifts in lake N:P stoichiometry and nutrient limitation driven by atmospheric nitrogen deposition. Science 6:835–837

Evans CD, Reynolds B, Jenkins A, Helliwell RC, Curtis CJ, Goodale CL, Ferrier RC, Emmett BA, Pilkington MG, Caporn SJM, Carroll JA, Norris D, Davies J, Coull MC (2006) Evidence that soil carbon pool determines susceptibility of semi-natural ecosystems to elevated nitrogen leaching. Ecosystems 9:453–462

Evans CD, Jones TG, Burden A, Ostle N, Zieliński P, Cooper MDA, Peacock M, Clark JM, Oulehle F, Cooper D, Freeman C (2012) Acidity controls on dissolved organic carbon mobility in organic soils. Glob Change Biol 18(11):3317–3331

Gerke J. (2010) Humic (organic matter)-Al(Fe)-phosphate complexes: An underestimated phosphate form in soils and source of plant-available phosphate. Soil Sci 175(9):417–425

Gerson JR, Driscoll CT, Roy KM (2016) Patterns of nutrient dynamics in Adirondack lakes recovering from acid deposition. Ecol Appl 26(6):1758–1770

Gislason SR, Oelkers EH, Eiriksdottir ES, Kardjilov MI, Gisladottir G, Sigfusson B, Snorrason A, Elefsen S, Hardardottir J, Torssander P, Oskarsson N (2009) Direct evidence of the feedback between climate and weathering. Earth Planet Sc Lett 277:213–222

Guidry MW, Mackenzie FT (2003) Experimental study of igneous and sedimentary apatite dissolution: control of pH, distance from equilibrium, and temperature on dissolution rates. Geochim Cosmochim Ac 67:2949–2963

Goodale CL, Aber JD, McDowell WH (2000) Long-term effects of disturbance on organic and inorganic nitrogen export in the White Mountains, New Hampshire. Ecosystems 3:433–450

Hall K. (2004) Evidence for freeze-thaw events and their implications for rock weathering in north Canada. Earth Surf Proc Land 29:43–57

Homyak PM, Sickman JO, Melack JM (2014) Pools, transformations, and sources of P in high-elevation soils: Implications for nutrient transfer to Sierra Nevada lakes. Geoderma 217−218:65−73

Huser BJ, Futter MN, Wang R, Fölster J (2018) Persistent and widespread long-term phosphorus declines in Boreal lakes in Sweden. Sci Total Environ 613–614:240–249

Kelly CA., Rudd JWM, Hesslein RH, Schindler DW, Dillon PJ, Driscoll CT, Gherini SA, Hecky RE (1987) Prediction of biological acid neutralization in acid-sensitive lakes. Biogeochemistry 3:129–140

Kaňa J, Kopáček J, Camarero L, Garcia-Pausas J (2011) Phosphate sorption characteristics of European alpine soils. Soil Sci Soc Am J 75:862–870

Kopáček J, Kaňa J, Šantrůčková H, Picek T, Stuchlík E. (2004) Chemical and biochemical characteristics of alpine soils in the Tatra Mountains and their correlation with lake water quality. Water Air Soil Pollut 153:307–327

Kopáček J, Stuchlík E, Wright RF (2005) Long-term trends and spatial variability in nitrate leaching from alpine catchment-lake ecosystems in the Tatra Mountains (Slovakia-Poland). Environ Pollut 136:89–101

Kopáček J, Hejzlar J, Vrba J, Stuchlík E (2011) Phosphorus loading of mountain lakes: Terrestrial export and atmospheric deposition. Limnol Oceanogr 56(4):1343–1354

Kopáček J, Hejzlar J, Kaňa J, Norton SA, Stuchlík E (2015a) Effects of acidic deposition on in-lake phosphorus availability: A lesson from lakes recovering from acidification. Environ Sci Technol 49:2895–2903

Kopáček J, Bičárová S, Hejzlar J, Hynštová M, Kaňa J, Mitošinková M, Porcal P, Stuchlík E, Turek J (2015b) Catchment biogeochemistry modifies long-term effects of acidic deposition on chemistry of mountain lakes. Biogeochemistry 125:315–335

Kopáček J, Kaňa J, Bičárová S, Fernandez IJ, Hejzlar J, Kahounová M, Norton SA, Stuchlík E (2017) Climate change increasing calcium and magnesium leaching from granitic alpine catchments. Environ Sci Technol 51(1):159–166

Křeček J, Palán L, Stuchlík E (2019) Impacts of land use policy on the recovery of mountain catchments from acidification. Land Use Policy 80:439–448

Mast MA, Turk JT, Clow DW, Campbell DH (2011) Response of lake chemistry to changes in atmospheric deposition and climate in three high-elevation wilderness areas of Colorado. Biogeochemistry 103:27–43

Matsuoka M, Murton J (2008) Frost weathering: Recent advances and future directions. Permafrost Periglac 19:195–210

Millot R, Gaillardet J, Dupré B, Allégre CJ (2002) The global control of silicate weathering rates and the coupling with physical erosion: new insights from rivers of the Canadian Shield. Earth Planet Sci Lett 196:83–98

Monteith DT, Stoddard JL, Evans CD, de Wit HA, Forsius M, Høgåsen T, Wilander A, Skjelkvåle BL, Jeffries DS, Vuorenmaa J, Keller B, Kopáček J, Veselý J (2007) Dissolved organic carbon trends resulting from changes in atmospheric deposition chemistry. Nature 450:537–540

Morales-Baquero R, Pulido-Villena E, Reche I (2006) Atmospheric inputs of phosphorus and nitrogen to the southwest Mediterranean region: Biogeochemical responses of high mountain lakes. Limnol Oceanogr 51:830–837

Moser KA, Baron JS, Brahney J, Oleksy I, Saros JE, Hundey EJ, Sadro SA, Kopáček J, Sommaruga R, Kainz MJ, Strecker AL, Chandra S, Walters DM, Preston DL, Michelutti N, Lepori F, Spaulding SA, Christianson K, Melack JM, Smol JP (2019) Mountain lakes: Eyes on global environmental change. Global Planet Change 178:77–95

Murphy J, Riley JP (1962) A modified single-solution method for the determination of phosphate in natural waters. Analyt chim Acta 27:31–36

Norton SA, Kahl JS, Henriksen A, Wright RF (1990) Buffering of pH depressions by sediments in streams and lakes. In: Norton SA, Lindberg SE, Page AL (eds) Acidic Precipitation. Advances in Environmental Science, vol 4. Springer, New York, pp 133–157

Oulehle F, Kopáček J, Chuman T, Černohous V, Hůnová I, Hruška J, Krám P, Lachmanová Z, Navrátil T, Štěpánek P, Tesař M, Evans DC (2016) Predicting sulphur and nitrogen deposition using a simple statistical method. Atmos Environ 140:456–468

Patrick WH, Khalid RA (1974) Phosphate release and sorption by soils and sediments. Science 186:53–55

Psenner R (1999) Living in a dusty world: Airborne dust as a key factor for alpine lakes. Water Air Soil Pollut 112:217–227

R Development Core Team (2015) R: A language and environment for statistical computing. R Foundation for Statistical Computing, Vienna

Riebe CS, Kirchner JW, Finkel RC (2004) Sharp decrease in long-term chemical weathering rates along an altitudinal transect. Earth Planet Sci Lett 218:421–434

Rogora M, Colombo L, Lepori F, Marchetto A, Steingruber S, Tornimbeni O (2013) Thirty years of chemical changes in alpine acid-sensitive lakes in the Alps. Water Air Soil Pollut 224:1746–1765

Schiff SL, Anderson RF (1986) Alkalinity production in epilimnetic sediments: Acidic and non-acidic lakes. Water Air Soil Pollut 31:941–948

Seidl R, Thom D, Kautz M, Martin-Benito D, Peltoniemi M, Vacchiano G, Wild J, Ascoli D, Petr M, Honkaniemi J, Lexer MJ, Trotsiuk V, Mairota P, Svoboda M, Fabrika M, Nagel TA, Reyer CPO (2017) Forest disturbances under climate change. Nat Clim Change 7:395–402

Smith EA, Mayfield CI, Wong PTS (1978) Naturally occurring apatite as a source of ortho-phosphate for growth of bacteria and algae. Microb Ecol 4(2):105–117

Stoddard JL, Van Sickle J, Herlihy AT, Brahney J, Paulsen S, Peck DV, Mitchell R, Pollard AI (2016) Continental-scale increase in lake and stream phosphorus: Are oligotrophic systems disappearing in the United States? Environ Sci Technol 50:3409−3415

Stuchlík E, Bitušík P, Hořická Z, Hardekopf D, Kahounová M, Tátosová J, Vondrák D, Dočkalová K (2017) Complexity in the biological recovery of Tatra Mountain lakes from acidification. Water Air Soil Pollut 228(5):184

Tipping E, Benham S, Boyle JF, Crow P, Davies J, Fischer U, Guyatt H, Helliwell R, Jackson-Blake L, Lawlor AJ, Monteith DT, Rowe EC, Toberman H (2014) Atmospheric deposition of phosphorus to land and freshwater. Environ Sci-Proc Imp 16:1608–1617

Thies H, Nickus U, Mair V, Tessadri R, Tait D, Thaler B, Psenner R (2007) Unexpected response of high alpine lake waters to climate warming. Environ Sci Technol 41:7424–7429

Thies H, Nickus U, Tolotti M, Tessadri R, Krainer K (2013) Evidence of rock glacier melt impacts on water chemistry and diatoms in high mountain streams. Cold Reg Sci Technol 96:77–85

Tsugeki NK, Agusa T, Ueda S, Kuwae M, Oda H, Tanabe S, Tani Y, Toyoda K, Wang W, Urabe J (2012) Eutrophication of mountain lakes in Japan due to increasing deposition of anthropogenically produced dust. Ecol Res 27:1041–1052

Vicars WC, Sickman JO (2011) Mineral dust transport to the Sierra Nevada, California: Loading rates and potential source areas. J Geophys Res-Biogeo 116:G01018

Wallander H, Wickman T, Jacks G (1997) Apatite as a P source in mycorrhizal and non-mycorrhizal *Pinus sylvestris* seedlings. Plant Soil 196:123–131

Welch SA, Taunton AE, Banfield JF (2002) Effect of microorganisms and microbial metabolites on apatite dissolution. Geomicrobiol J 19:343–367

White AF, Schulz MS, Lowenstern JB, Vivit DV, Bullen TD (2005) The ubiquitous nature of accessory calcite in granitoid rocks: Implications for weathering, solute evolution, and petrogenesis. Geochim Cosmochim Ac 69:1455–1471

Wolfe AP, Baron JS, Cornett RJ (2001) Anthropogenic nitrogen deposition induces rapid ecological changes in alpine lakes of the Colorado Front Range (USA). J Paleolimnol 25:1–7

Table 1. Chemical composition[1] of extracts from crushed granodiorite samples G1 to G12 with diluted HNO_3 (original pH of 3.5). Values are cumulative for 15 consecutive extraction steps (24-hour each, 20–25 °C).

		G1	G2	G3	G4	G5	G6	G7	G8	G9	G10	G11	G12
pH		5.41	3.69	4.89	4.30	4.37	3.89	3.65	3.60	4.80	3.92	5.97	4.38
HCO_3^-	$\mu mol\ g^{-1}$	4.4	0.0	2.9	0.1	0.5	0.0	0.0	0.0	3.4	0.0	8.5	2.1
H^+	$\mu mol\ g^{-1}$	23.3	7.6	22.8	16.2	16.6	11.5	5.7	4.8	22.5	14.8	23.6	20.6
Ca	$\mu mol\ g^{-1}$	14.4	1.7	13.8	6.2	7.3	3.6	1.7	0.7	10.3	5.5	13.7	9.7
Mg	$\mu mol\ g^{-1}$	0.2	0.2	0.1	0.4	0.4	0.5	0.1	0.0	0.2	0.4	0.1	0.2
Na	$\mu mol\ g^{-1}$	0.6	0.6	0.5	0.7	0.6	0.6	0.4	0.5	0.5	0.5	0.5	0.4
K	$\mu mol\ g^{-1}$	0.4	0.5	0.6	1.4	0.9	1.5	0.4	0.5	0.6	0.8	0.4	0.5
SRP	$\mu mol\ g^{-1}$	0.08	0.75	0.21	0.41	0.85	1.31	0.79	0.27	0.23	0.98	0.12	0.13
SRP:TP	%	0.5	6.2	3.0	2.6	4.5	7.7	7.2	2.9	1.6	5.8	0.6	1.5
Apatite Ca:P	molar	1.56	1.54	1.51	1.64	1.66	1.65	1.64	1.66	1.65	1.68	1.64	1.64
Apatite-Ca	$\mu mol\ g^{-1}$	0.12	1.16	0.32	0.67	1.40	2.17	1.29	0.44	0.38	1.65	0.19	0.22

[1]pH is the average pH of extraction solution for 15 extractions, computed from H^+ concentrations at the end of each extraction; HCO_3^- is equal to positive values of ANC; H^+ is amount of protons neutralized during extractions (the sum of the differences between the initial and final H^+ concentrations during individual extractions); Ca, Mg, Na, and K are sums of dissolved metals; SRP is sum of extracted soluble reactive phosphorus; SRP:TP is percent of P in the form of SRP in the samples; apatite Ca:P is molar ratio of these elements in apatite in the granodiorite samples (Table SM-5); and apatite-Ca is amount of Ca extracted from apatite. Amounts of Al, Fe, and Si extracted during the 15 extractions were small (< 0.03, < 0.004, and $< 0.5\ \mu mol\ g^{-1}$, respectively) and are not shown.

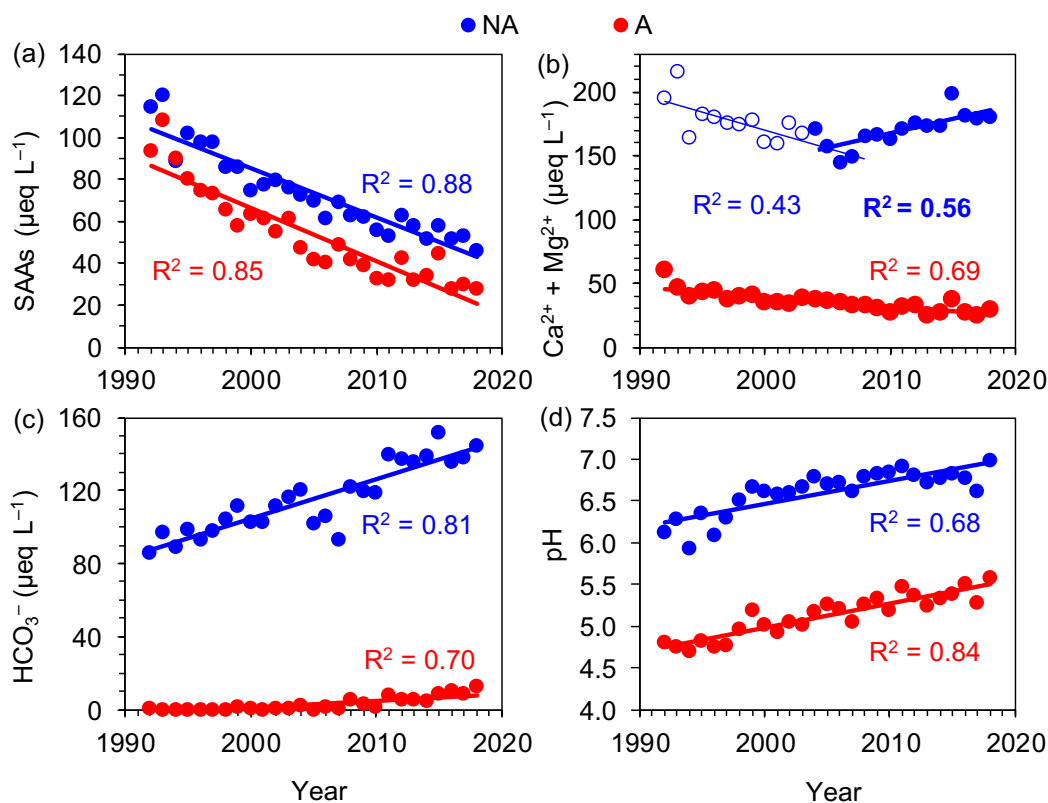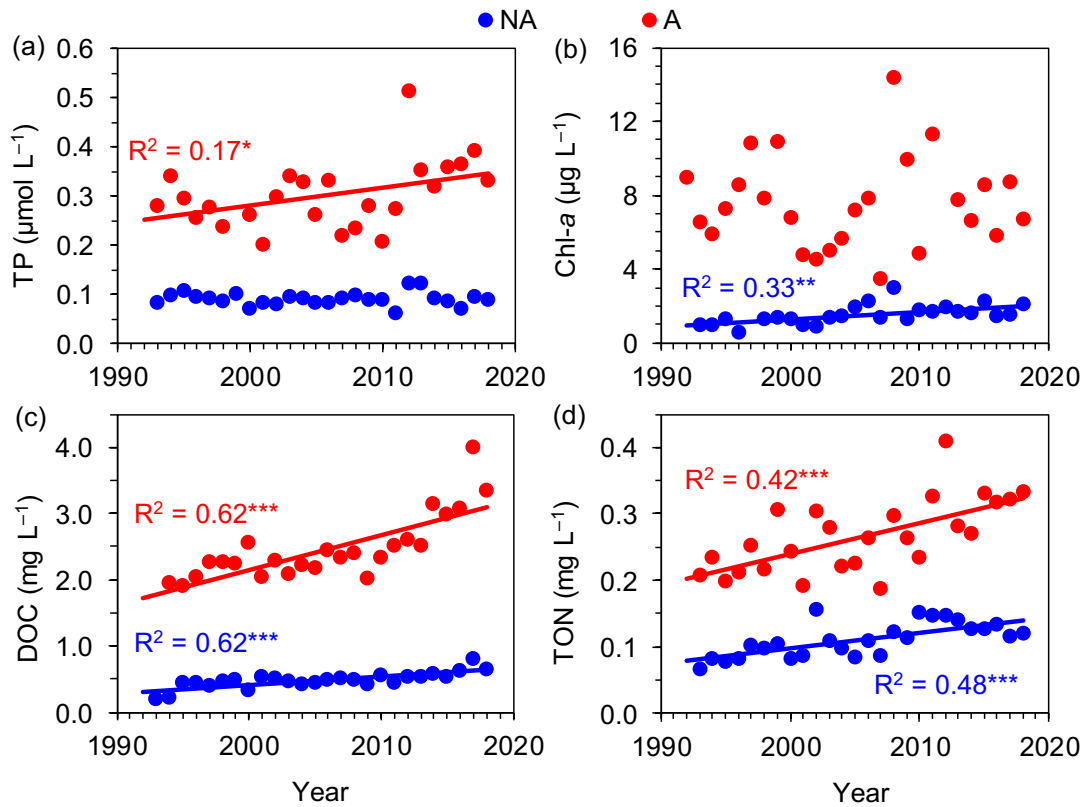Fig. 1. Time series (1992–2018) for average ionic water concentrations for non-acidic (NA, n = 25, blue symbols) and acidic (A, n = 6, red symbols) lakes in the Tatra Mountains: (a) strong acid anions (SAAs = sum of SO_4^{2-}, NO_3^- and Cl^- concentrations), (b) sum of (Ca^{2+} + Mg^{2+}) concentrations, (c) HCO_3^-, and (d) pH. R^2 is coefficient of determination ($p < 0.001$ for all relationships given by solid lines). Trend of (Ca^{2+} + Mg^{2+}) concentrations is divided into the 1992–2003 and 2004–2018 periods according to Kopáček et al. (2017). For τ-values and significance of Mann-Kendall test see Table SM-9.

Fig. 2. Time series (1992–2018) for average ionic water concentrations in non-acidic (NA, n = 25, blue symbols) and acidic (A, n = 6, red symbols) lakes in the Tatra Mountains: (a) total phosphorus (TP), (b) chlorophyll *a* (Chl-*a*), (c) dissolved organic carbon (DOC), and (d) total organic nitrogen (TON). R^2 is coefficient of determination and asterisks indicate significance of relationship (*, $p < 0.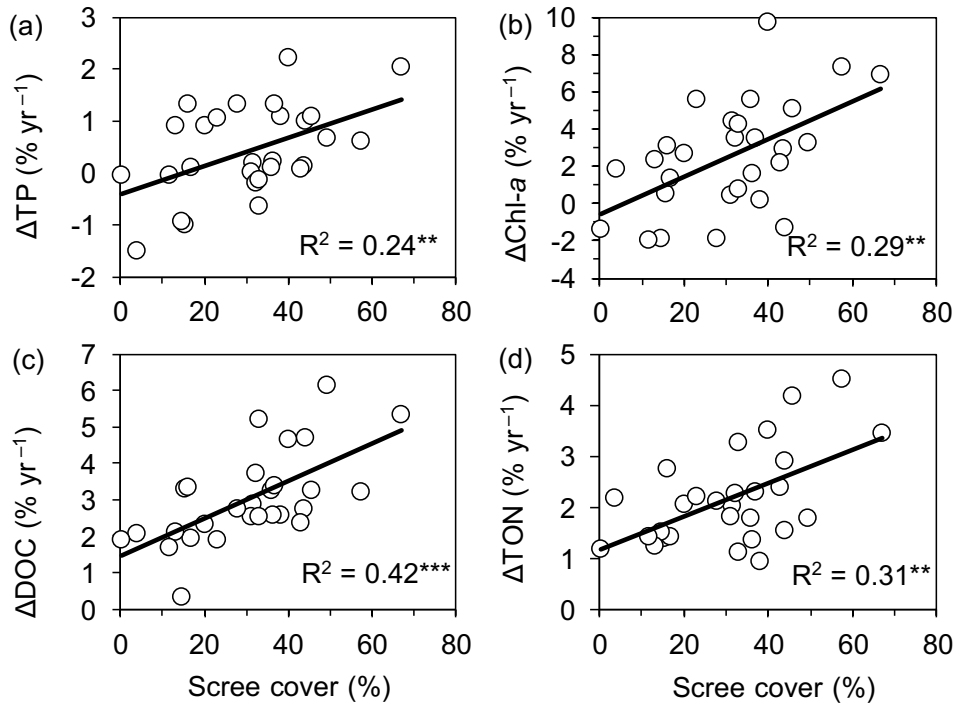05$; **, $p < 0.01$; ***, $p < 0.001$) given by solid lines. For τ-values and significance of Mann-Kendall test see Table SM-9.
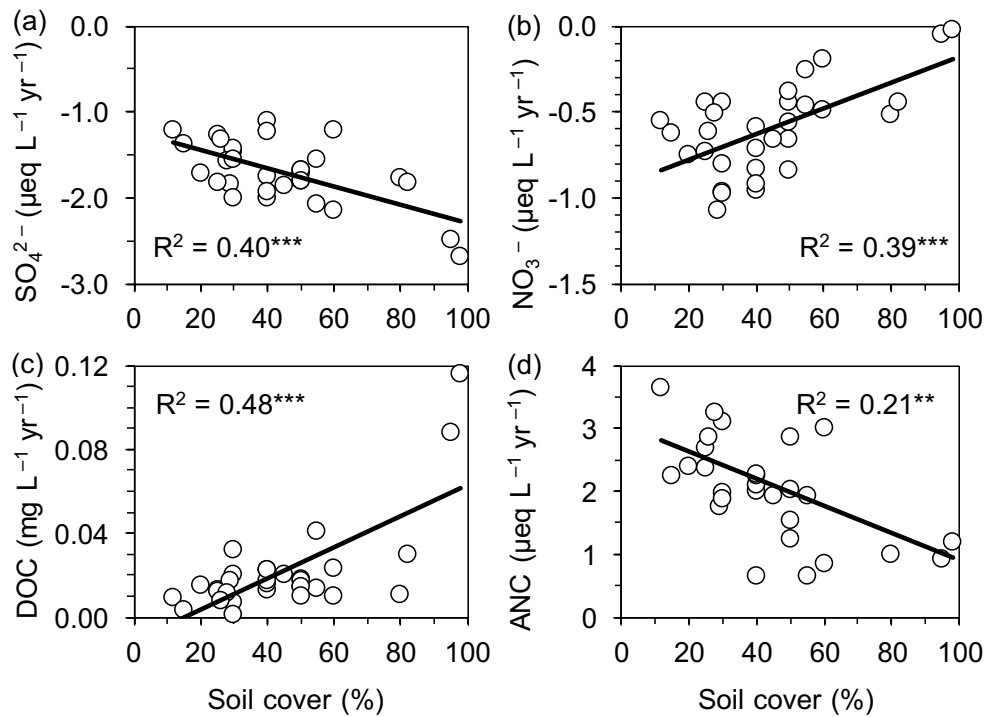
Fig. 3. Relationships between percentage catchment cover with soil (meadows, dwarf pine, and spruce forest) *versus* slopes of changes in solute concentrations in the Tatra Mountain lakes during 1992–2018: (a) SO_4^{2-}, (b) NO_3^-, (c) dissolved organic carbon (DOC), and (d) acid neutralizing capacity (ANC). R^2 is coefficient of determination and asterisks indicate significance of relationship (**, $p < 0.01$; ***, $p < 0.001$) given by solid lines.

Fig. 4. Relationships between percentage catchment cover with scree areas *versus* percentage changes of absolute concentrations (Δ) in the Tatra Mountain lakes during 1992–2018: (a) total phosphorus (TP), (b) chlorophyll *a* (Chl-*a*), (c) dissolved organic carbon (DOC), and (d) total organic nitrogen (TON). All concentrations were normalized to their average concentrations during this period. R^2 is coefficient of determination and asterisks indicate significance of relationship (**, $p < 0.01$; ***, $p < 0.001$) given by solid lines.
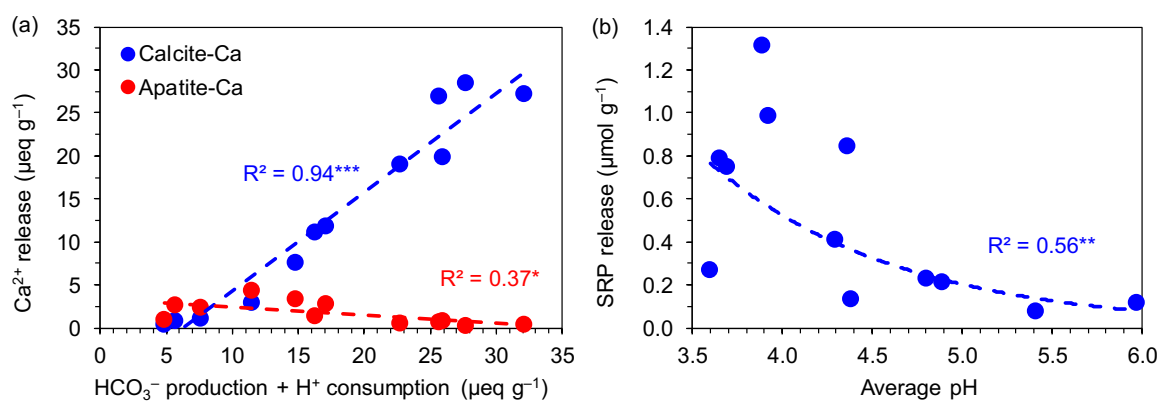
Fig. 5. Relationship between (a) dissolved carbonate (HCO_3^- production plus H^+ consumption) and Ca originating from calcite (calcite-Ca) and apatite (apatite-Ca), and (b) average pH of extraction solution and soluble reactive phosphorus (SRP) extracted from 12 Tatra Mountain granodiorite rocks (Table SM-3). All values are cumulative values for 15 consecutive extraction steps with diluted HNO_3 (0.32 mmol L^{-1}; original pH of 3.5), except for average pH (calculated from average H^+ concentration at the end of each step). Equation of relationship given in Fig. 5b is $SRP = 23.4e^{-0.95pH}$. R^2 is coefficient of determination and asterisks indicate significance of relationship (*, $p < 0.05$; **, $p < 0.01$; ***, $p < 0.001$) given by lines.
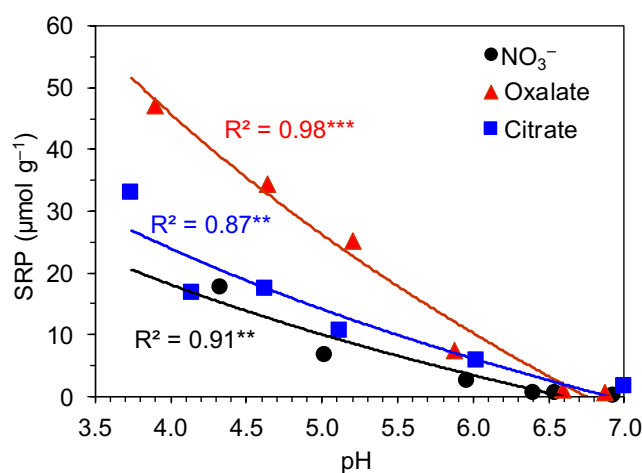

Fig. 6. Effect of pH (final pH of extraction solution) on release of soluble reactive phosphorus (SRP) from apatite (sample A1) during a single 24-hour extraction with 0.32 mmol HNO_3 L^{-1}, and oxalic and citric acid (both 1 mmol L^{-1}). Initial solutions were titrated with NaOH to starting pH values of 3.5, 4, 4.5, 5, 6, and ~7. R^2 is coefficient of determination and asterisks indicate significance of relationship (**, $p < 0.01$; ***, $p < 0.001$) given by solid lines.

21

Supplementary Material to

Climate change accelerates recovery of the Tatra Mountain lakes from acidification and increases their nutrient and chlorophyll *a* concentrations

Jiří Kopáček[*,1,2], Jiří Kaňa[1,2], Svetlana Bičárová[3], Janice Brahney[4], Tomáš Navrátil[5], Stephen A. Norton[6], Petr Porcal[1,2], Evžen Stuchlík[1]

[1]Biology Centre CAS, Institute of Hydrobiology, CZ-370 05 České Budějovice, Czech Republic
(*E-mail of corresponding author: jkopacek@hbu.cas.cz)
[2]University of South Bohemia, Faculty of Science, CZ-370 05 České Budějovice, Czech Republic
[3]Earth Science Institute, Slovak Academy of Sciences, 059 60 Tatranská Lomnica, Slovak Republic
[4]Utah State University, Department of Watershed Sciences, 5210 Old Main Hill, Logan, USA
[5]Institute of Geology CAS, CZ-165 00 Prague 6, Czech Republic.
[6]Earth and Climate Sciences, University of Maine, Orono, Maine 04469, USA

(Supplementary Material includes 7 pages, 3 figures, and 9 tables)

Part SM-1: Details to section: Methods
Physical and hydrological characteristics of lakes and their catchments and details on lake water sampling and analysis.

Table SM-1. Major physical and hydrological characteristics for the 31 Tatra Mountain catchment-lake systems used in this study. Data are from Kopáček et al. (2017).

Lake name	Lake code	Latitude (°N)[a]	Longitude (°E)[a]	Elevation (m)	Volume (10^3 m³)	Maximum depth (m)	Lake area (ha)	Retention time (yr)	Catchment area (ha)	Maximum relief (m)	Bedrock (%)	Scree area (%)	Soil[b] cover (%)	Fish[c]
Batizovské	BA-01	49.152	20.130	1884	173	10.5	3.48	0.05	234	775	33	57	10	No
Litvorové	BV-03	49.177	20.129	1860	135	19.1	1.86	0.16	62.7	566	39	44	17	No
Vyšné Žabie bielovodské	BV-22	49.194	20.093	1699	839	24.8	9.46	0.60	101.4	564	46	16	38	No
Vyšné Wahlenbergovo♣	FU-01	49.164	20.026	2157	392	20.6	5.17	0.93	32	259	50	46	4	No
Nižné Wahlenbergovo♣	FU-04	49.159	20.025	2053	71	7.8	2.03	0.06	69.8	360	43	49	8	No
Vyšné Furkotské	FU-07	49.144	20.030	1698	3.3	2.4	0.41	0.05	13.7	182	1	4	95	No
Długi Staw Gąsienicowy	GA-04	49.227	20.009	1784	81	10.6	1.59	0.09	65	517	28	40	32	No
Zielony Staw Gąsienicowy	GA-07	49.229	20.000	1672	261	15.1	3.84	0.65	33	419	15	17	68	T.
Veľké Hincovo	ME-01	49.179	20.059	1945	4092	54.0	20.08	2.5	127	486	39	32	29	T.
Malé Hincovo	ME-02	49.174	20.057	1921	72	6.4	2.23	0.29	21	277	6	38	56	No
Vyšné Satanie*	ME-04	49.170	20.061	1894	2.5	3.5	0.20	0.05	2.1	80	3	36	61	No
Czarny Staw pod Rysami	MO-01	49.189	20.078	1580	7762	76.4	20.64	3.4	179	920	61	15	24	T.
Morskie Oko	MO-02	49.198	20.072	1395	9935	50.8	34.93	1.3	630	1105	36	20	44	T.
Wyżni Mnich. Staw IX*	MO-06	49.194	20.054	1870	0.46	2.3	0.06	0.02	1.7	50	27	37	37	No
Veľké spišské	MS-04	49.193	20.195	2013	125	10.1	2.87	0.08	123.5	613	23	67	10	No
Vyšné Terianske*	NE-01	49.168	20.021	2124	8.5	4.3	0.56	0.03	19	319	53	41	6	No
Nižné Terianske	NE-03	49.170	20.013	1940	872	47.3	5.56	0.57	110	487	46	44	10	No
Czarny Staw Polski	PS-02	49.205	20.028	1722	2826	50.4	12.69	3.89	60.4	333	16	31	53	T.
Wielki Staw Polski	PS-03	49.211	20.042	1655	12967	79.3	34.35	2.1	491	646	12	36	51	T.
Vyšné Račkove	RA-01	49.200	19.805	1697	27	12.3	0.74	0.05	56	440	5	23	72	B.
Štvrté (Horné) Roháčske	RO-01	49.206	19.736	1719	46	8.2	1.44	0.29	14	302	37	16	47	No
Prvé (Dolné) Roháčske	RO-04	49.207	19.743	1562	77	7.7	2.23	0.16	43.6	457	5	13	82	No
Slavkovské*	SL-02	49.153	20.183	1676	1.1	2.5	0.11	0.02	5.1	34	0	5	95	No
Jamské*	ST-01	49.133	20.012	1448	11	4.3	0.68	0.10	12.7	133	0	0	100	No
Vyšné Temnosmrečinské	TE-01	49.189	20.038	1725	415	20.0	5.56	0.33	112	662	44	33	23	No
Nižné Temnosmrečinské	TE-03	49.193	20.029	1677	1502	38.1	11.70	0.82	215.0	704	33	28	39	No
Zelené krivánske	VA-01	49.159	20.008	2013	289	29.5	5.14	0.40	59.0	478	58	32	9	No
Pusté♣	VS-02	49.182	20.154	2056	32	6.6	1.19	0.15	20.4	328	17	43	40	No
Ľadové♣	VS-04	49.184	20.161	2057	101	18.0	1.74	0.66	13	293	8	64	28	No
Starolesnianske*	VS-15	49.180	20.167	1988	11	4.2	0.72	0.41	2.3	44	10	12	78	No
Veľké Žabie	ZA-03	49.172	20.077	1921	74	7.0	2.65	0.06	86.7	581	33	33	34	No

[a]All coordinates used in this study refer to the World Geodetic System, 1984 (WGS84).
[b]Soil in alpine meadows and areas covered with dwarf pine (*Pinus mugo*) or Norway spruce (*Picea abies*).
[c]Abbreviation No = no fish; T. = trout; B. = bullhead.
*Acidic lakes, with average HCO_3^- < 20 μeq L⁻¹ between 1992 and 2018.
♣Catchments with sampled rocks.

Soil chemistry: Data on soil amounts and chemistry in catchments of the Tatra Mountain lakes are from Kopáček et al. (2004, 2015a). Depth and amount of fine soil (dry weight, <2 mm soil fraction) ranged from 0.1 to 0.84 m and from 38 to 255 (121 on average) kg m⁻², respectively, in alpine meadows, and its average loss on ignition at 550 °C was 15%. The till soils formed thin (<3 cm deep) layers or lenses of finer-grained material between boulders in the scree areas below a 20–80 cm thick layer of surface stones; its fine fraction ranged between 4–33 (13 on average) kg m⁻². Soil TP concentrations in alpine meadows averaged (± standard deviation) 31±11 and 21±9 μmol g⁻¹ in the organic and mineral soil horizons, respectively, with the mass weighted mean for alpine

meadows of 25 ± 10 µmol g^{-1}. Even though TP concentrations were only slightly higher in till soils (35 ± 8 µmol g^{-1}) than in meadow soils, they had about 3-times higher concentrations of oxalate extractable SRP 12 ± 4 *vs.* 3.6 ± 1.6 µmol g^{-1}) despite their lower phosphate adsorbing capacity. This capacity was inferred from concentrations of Al and Fe hydroxides, determined by oxalate extraction (Al$_{ox}$ and Fe$_{ox}$). The respective concentrations of Al$_{ox}$ and Fe$_{ox}$ averaged 111 and 58 µmol g^{-1} in till soils and 194 and 80 µmol g^{-1} in alpine meadow soils. Soils were acidic, with pH$_{H2O}$ in the range of 4–5 and average values of 4.5 ± 0.1 and 4.6 ± 0.2 for the till and alpine meadow soils, respectively (Kopáček et al. 2004).

Climate characteristics: Data on daily precipitation, snow cover, and minimum, maximum and average air temperature in the Tatra Mountains were measured at the Meteorological observatory Skalnaté Pleso (20.234 °E, 49.189 °N, elevation of 1778 m, operated by Earth Science Institute of Slovak Academy of Sciences). Data analysis was performed as described by Kopáček et al. (2017) for the 1965–2018 period (Fig. SM-1).
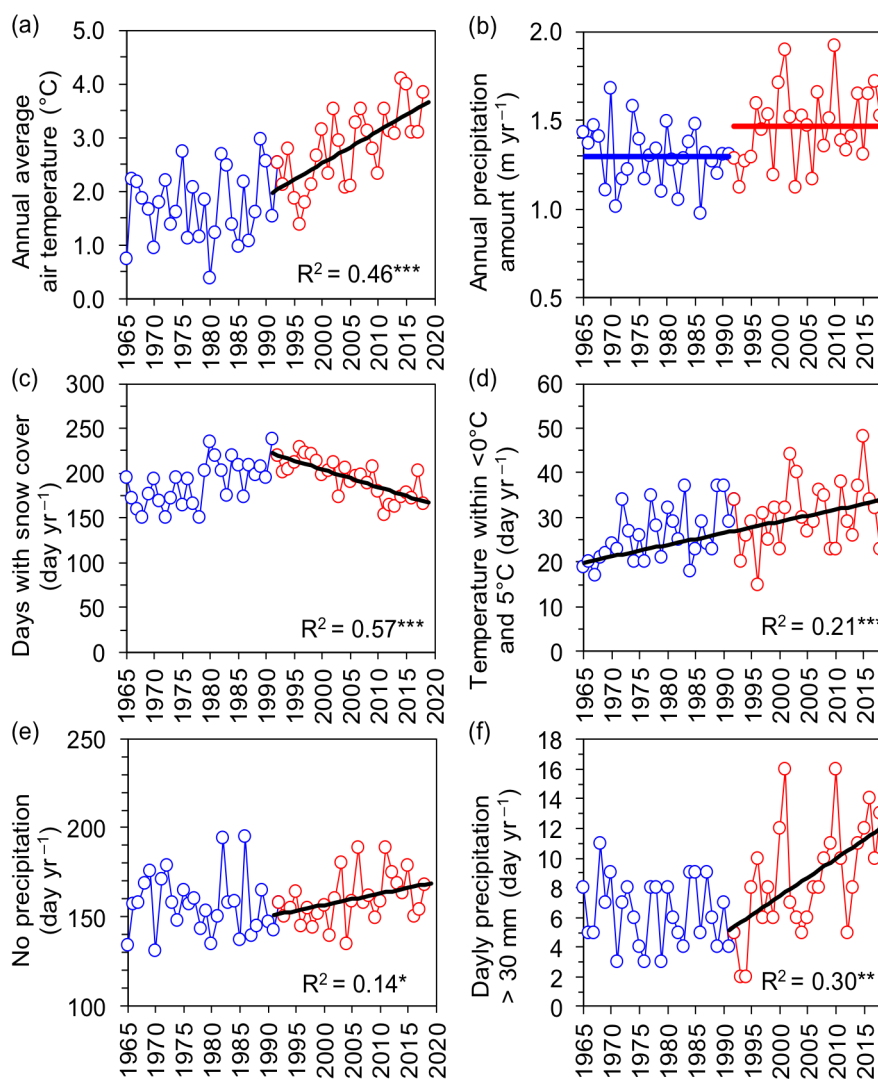

Fig. SM-1. Time series of climate characteristics from the Tatra Mountain Skalnaté Pleso meteorological observatory, elevation of 1778 m: (a) Annual average air temperature; (b) annual precipitation amount; (c) number of days with snow cover > 2 cm, (d) minimum air temperature below 0 °C and maximum air temperature above 5 °C, (e) no precipitation, and (f) precipitation amount > 30 mm day^{-1}. Blue and red points represent the 1965–1991 and 1992–2018 periods, respectively, and blue and red solid lines in panel (b) their averages (1.30 and 1.46 m yr^{-1}). Solid black lines in panels show significant linear regressions for the 1992–2018 period [except for panel (d), showing the 1965–2018 trend]; R^2 is coefficient of determination and asterisks indicate significance of relationship (***, $p<0.001$; **, $p<0.01$; and *, $p<0.05$).

Lake water sampling and analyses: Lake water samples were taken from the outflow or surface (5–20 cm depth) and were field-filtered through a 40 µm polyamide sieve to remove zooplankton and coarse particles. Samples were re-filtered with membrane filters (pore size of 0.45 µm) within 5–10 hours after sampling for the determination of ions, with glass-fibre filters (pore size of 0.4 µm) for dissolved organic carbon (DOC), and with Whatman GF/C filters for chlorophyll *a* (Chl-*a*). Samples for pH, acid neutralising capacity (ANC, determined by Gran titration), total phosphorus (TP), and total organic nitrogen (TON) were not filtered after the field pre-filtration. Samples for ion determination were frozen at –20 °C and other samples were stored in dark at 4 °C prior to analyses (< 2 weeks).

During 1992–2018, major base cations (Ca^{2+}, Mg^{2+}, Na$^+$, and K$^+$), NH$_4^+$, and strong acid anions (SO$_4^{2-}$, NO$_3^-$, and Cl$^-$) were determined by ion chromatography. The accuracy and precision of analytical methods were checked by means of standard samples, which were assayed with each series of samples. The accuracy of analyses was also checked using ion balance calculations for each sample (including aluminium forms and organic acids, Kopáček et al. 2000). For this ion balance control, positive values of measured ANC (Gran titration) were assumed to represent HCO$_3^-$ concentrations, and HCO$_3^-$ = 0 was used for all ANC values ≤ 0 µmol L^{-1}. The differences between the sum of cations and the sum of anions were < ±8% of the total ionic concentration for all samples. Concentration of Chl-*a* was determined fluorometrically, after extraction of the

Whatman GF/C filters in a hot mixture of 90% acetone and methanol (Fott et al. 1999). Details and detection limits of individual methods are in Table SM-2.

Table SM-2. Methods used for the determination of individual water constituents and their abbreviations.

Abbreviation	Explanation	Analytic method
ANC, HCO_3^-	Acid neutralizing capacity, bicarbonate	Gran titration (Tacussel in 1992–2011, then Radiometer). ANC = HCO_3^- for ANC >0 µmol L^{-1}; $HCO_3^- = 0$ for ANC ≤ 0 µmol.l^{-1}.
H^+ (pH)	Proton concentration	pH electrode (combined, Radiometer)
NH_4^+, Ca^{2+}, Mg^{2+}, Na^+, K^+, NO_3^-, Cl^-, SO_4^{2-}, F^-	Major cations and anions	Ion chromatography (Thermo Separation Products in 1992–2000, Dionex IC25 in 2001–2011, then Dionex ICF-3000). Detection limits for ions were 0.1–0.4 µmol L^{-1}.
Si	Dissolved reactive silica	Molybdate method (Golterman and Clymo 1969).
DOC	Dissolved organic carbon	LiquiTOC analyser (Foss-Heraeus, Germany) in 1992–1999 and Shimadzu analysers TOC 5000A in 2000–2015 and then TOC-L; detection limit of <0.05 mg L^{-1}.
TON	Total organic nitrogen	Kjeldahl digestion (Procházková 1960); detection limit of ~2 µmol L^{-1} (~25 µg L^{-1}).
TP	Total phosphorus	Sample pre-concentration, $HClO_4$ digestion, molybdate method (Kopáček and Hejzlar 1993); detection limit of 0.015 µmol L^{-1} (~0.5 µg L^{-1}).
Chl-*a*	Chlorophyll *a*	Fluorometric method, extraction in hot mixture of acetone and methanol (Fott et al. 1999), detection limit of ~0.01 µg L^{-1}.
Al_d, Al_i, Al_o	Dissolved, ionic, and organically-bound aluminium	Fractionation according to Driscoll (1984), colorimetry (Dougan and Wilson 1974) throughout 1992–2018; detection limit of 0.1 µmol L^{-1}. $Al_i = Al_d - Al_o$.

Part SM-2: Details to section: Methods
Extraction experiments with granodiorite bedrock

Samples of the dominant granodiorite bedrock (G1 to G12) were taken from catchments of lakes FU-01, FU-04, VS-02, and VS-04 (Table SM-1). Samples G1, G2, and G3 were identical to the A, B, and C samples, respectively, from the previous study (Kopáček et al. 2017). We carefully cut off ~5–10 cm thick rind of weathered surface and used the unweathered material for further analyses and experiments. The samples were analysed for total chemical composition at the Czech Geological Survey (Table SM-3) and for mineral content at the Institute of Geology, Czech Academy of Science (Table SM-4). The mineral content was estimated using the Bruker D8 Discover X-ray powder diffraction diffractometer equipped with a silicon-strip linear LynxEye detector and a focusing germanium primary monochromator of Johansson type providing CuKα1 radiation (λ = 1.54056 Å). Data for mineral identification were collected in the 2θ range of 5–80° with a step size of 0.016° and a counting time of 1 second at each step, and detector angular opening of 2.935°. The phase identification was performed with Diffrac. Eva software v4.3.0.1 and ICDD PDF-2 database (Bruker AXS GmbH, Karlsruhe, Germany; 2011–2018). Semi-quantitative estimation of the mineral composition was calculated by the reference intensity ratio method implemented in Diffrac.Eva software. Chemical compositions of apatite (Table SM-5) and its Ca:P ratios in the granodiorite samples were determined by electron probe micro analyser (CAMECA SX-100) at the Institute of Geology, Czech Academy of Science. Accelerating voltage was adjusted to 15 kV, sample current to 10 nA, and beam diameter set to 2 µm. The standards used were: apatite (Ca, P), jadeite (Na), obsidian (Si), barite (S), rhodonite (Mn), fluorite (F), tugtupite (Cl) and celestite (Sr). All elements were analysed on Kα spectral lines, except for Sr which was analysed on Lα line. Crushed samples were sieved. The 2–5 mm fraction (selected on a basis of previous experiments; Kopáček et al. 2017) was used in laboratory experiments after washing with distilled water to remove rock dust. The sample of apatite (A1) was from the collection of Institute of Geology. It was crushed, sieved, and analysed identically to the granodiorite samples.

Experiment 1 (12 granodiorite samples, initial pH of 3.5): We measured total amount of neutralized H^+ and released HCO_3^-, major metals (Ca, Mg, Na, K, Al, Fe), silicon (Si), and soluble reactive phosphorus (SRP) from rocks during each 24-hour extraction step with HNO_3 diluted with deionized water to initial pH = 3.5. All extractions were done in 100-ml polyethylene centrifugation tubes on a horizontal shaker, with the rock to water mass ratio of 1:5 at 20–25 °C. After extraction, samples were filtered (pore size of 0.4 µm type GF-5, Macherey-Nagel, Düren, Germany), filtrate was used for analyses, and the remaining rock sample was extracted again with the same volume with a fresh solution. This step was repeated 15 times on the basis of previous experiments (Kopáček et al. 2017), i.e., until negative ANC values occurred in samples after the 24-hour extraction.

   All experiments were done in triplicate and averages were used for data evaluation. The amount of neutralized H^+ was computed from the difference between the initial and final pH during individual extractions. Concentrations of released Ca, Mg, Na, K, Al, Fe, and Si were analysed using ICP-MS (8800 Triple Quadrupole ICP-MS analyser, Agilent Technologies). Concentration of SRP was determined according to Murphy and Riley (1962). We did not analyse TP, because similar concentrations of SRP and TP in previous experiments with samples G1 to G3 (Kopáček et al. 2017) suggested phosphate re-adsorption on colloidal particles that formed during experiments (e.g. $Al(OH)_3$ hydroxide) was negligible and did not significantly affect the results.

Concentrations of HCO_3^- were measured as positive ANC values (Gran titration). Total amount of carbonate dissolved in rocks during extractions (either released as HCO_3^- or neutralized with H^+ to CO_2) was computed as the sum of the consumed H^+ (other possible H^+ consuming processes were neglected for simplicity) and measured HCO_3^-. Then, we computed cumulative amounts of metals, Si, SRP, and dissolved carbonate during the 15 extraction steps. Average pH of extraction solution for all 15 extraction steps was computed from average H^+ concentrations at the end of each step.

Experiment 2 (7 granodiorite samples, initial pH of 5.0): We selected three samples with the highest carbonate content (G1, G3, and G11) and four samples with the lowest carbonate content (G2, G6, G7, and G8) (Table SM-3) and extracted them repeatedly in 15 extraction steps with HNO_3 diluted with deionized water to initial pH = 5.0. Other experimental conditions and analyses were the same as in the *Experiment 1*.

Experiment 3 (apatite, initial pH of 3.5–6.8): We extracted 0.3–0.5 g of crushed apatite (2–5 mm fraction) for 24 hours at laboratory temperature with (1) HNO_3 (0.32 mmol L^{-1}; pH = 3.5) and NaOH solutions at initial pH values of 3.5, 4.0, 4.5, 5.0, 5.8 and 6.7; (2) 1 mM oxalic acid and NaOH at initial pH values of 3.5, 4.0, 4.5, 5.1, 6.0 and 6.8; and (3) 1 mM citric acid and NaOH at initial pH values of 3.5, 4.0, 4.5, 5.0, 5.9 and 6.9. Extracts were filtered as in *Experiment 1* and analysed for concentrations of dissolved Ca and P using ICP-MS.

Table SM-3. Chemical composition[1] of granodiorite samples G1 to G12. Units: µmol g^{-1}.

	G1	G2	G3	G4	G5	G6	G7	G8	G9	G10	G11	G12
Si	11599	11576	12276	11736	11578	11470	12294	12391	11728	11566	11614	11913
Al	3011	3067	2816	2784	3013	3204	2816	2741	2960	3009	3011	2883
Fe	308	309	133	379	329	316	88	108	289	303	287	214
Mn	6	6	5	10	8	7	3	7	8	7	8	7
Ti	44	43	14	51	48	46	9	9	40	41	39	28
Ca	436	454	170	246	552	529	145	121	445	484	430	352
Mg	208	208	87	261	221	213	52	60	196	223	194	166
Na	1455	1445	1239	1226	1458	1442	1103	1165	1413	1452	1419	1390
K	435	435	752	756	425	435	1008	924	497	484	495	690
Sr	6.9	7.0	2.6	3.3	7.0	7.0	2.1	2.4	6.7	7.3	5.7	6.1
Ba	7.2	8.2	6.1	7.9	8.1	8.1	4.1	6.7	8.5	9.8	8.1	11.1
Li	2.0	4.0	1.3	9.4	4.0	3.3	2.0	2.0	3.3	3.3	4.0	3.3
P	15	12	7	16	19	17	11	9	14	17	19	9
F	28	24	20	27	22	15	11	14	15	16	27	25
C[2]	64	<2.0	46	11	15	3.2	4.1	4.3	45	9	89	29

[1]Total chemical composition was determined after mineralization of finely ground samples with H_2SO_4, HNO_3, and HF (200°C, 2 hours). Metals were analysed by the flame atomic absorption spectrometry, except for Al (volumetric titration).
[2]Carbon was determined as CO_2 by infrared detection after acidifying ground sample with H_3PO_4.

Table SM-4. Mineral composition[1] of granodiorite samples G1 to G12. Units: %.

	G1	G2	G3	G4	G5	G6	G7	G8	G9	G10	G11	G12
Quartz	22	24	38	39	26	31	33	26	33	35	21	28
Plagioclase (Ca-Na-albite)	36	38	26	20	49	30	35	45	23	38	49	36
K-feldspar (Microcline)	5	15	8	12	5	20	7	13	18	6	9	16
Chlorite (Clinochlore)	15	6	2	6	10	4	11	5	5	3	4	4
Muscovite	19	15	24	13	5	12	15	11	16	10	12	11
Biotite	2	1	2	10	5	4			5	8	4	5

[1]Semi-quantitative estimation of the mineral composition was calculated by the reference intensity ratio method. Apatite and calcite contributions to the total mineral composition were traces (<0.5%).

Table SM-5. Composition[1] of apatite A1 and apatite traces in granodiorite samples G1 to G12. Units: mmol g^{-1}.

	G1	G2	G3	G4	G5	G6	G7	G8	G9	G10	G11	G12	A1
Ca	9.8	9.5	9.5	9.9	10.0	9.9	9.9	9.9	9.9	9.9	10.0	10.0	9.9
P	6.2	6.2	6.3	6.1	6.0	6.0	6.0	6.0	6.0	5.9	6.1	6.1	5.8
O	25.4	24.9	25.1	25.2	25.1	25.1	25.1	25.1	25.0	24.8	25.2	25.2	24.9
F	1.7	1.6	1.3	2.0	2.1	1.9	2.0	2.0	2.0	2.0	2.0	2.0	1.9

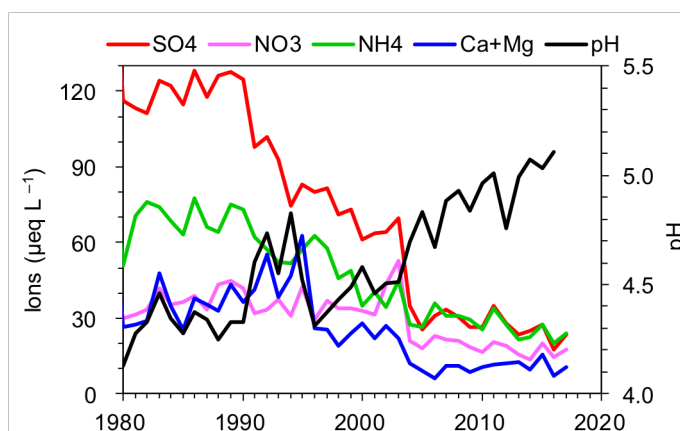[1]Chemical composition was determined by electron probe microprobe.

Fig. SM-2. Time series of chemical composition of bulk atmospheric deposition at Chopok meteorological station, situated in the Low Tatra Mountains at 19.590 °E, 48.944 °N, and elevation 2008 m (~50 km southwest of the central Tatra Mountains). Data by the Slovak Hydro-meteorological Institute (Mitošinková M. *pers. commun.*).

Table SM-6. Average chemical composition of the Tatra Mountain lakes from 1992–2018 (for lake codes see Table SM-1); sum of Ca^{2+} and Mg^{2+} (Ca+Mg), acid neutralizing capacity (ANC), total phosphorus (TP), chlorophyll *a* (Chl-*a*), total organic nitrogen (TON), dissolved organic carbon (DOC), and dissolved silicon (Si).

	Lake	pH[b]	Ca+Mg	SO_4^{2-}	NO_3^-	Cl^-	ANC	TP	Chl-*a*	TON	DOC	Si
			---------------- µeq L^{-1} yr^{-1} ----------------					------ µg L^{-1} yr^{-1} ------			-- mg L^{-1} yr^{-1} --	
Non–acidic lakes[a]	BA-01	6.35	109	45	35	4	42	1.58	0.62	67	0.21	1.06
	BV-03	6.86	197	44	24	4	131	2.20	0.89	101	0.27	0.87
	BV-22	6.48	120	48	20	4	51	1.96	0.90	114	0.55	0.69
	FU-01	6.40	103	30	25	4	52	2.93	1.09	97	0.28	0.48
	FU-04	6.49	113	33	28	4	59	2.84	1.43	119	0.33	0.73
	FU-07	6.47	108	48	23	5	56	4.91	0.74	130	0.51	1.62
	GA-04	6.16	92	44	31	4	27	1.96	0.74	86	0.37	0.91
	GA-07	6.77	142	42	13	5	100	4.05	6.74	151	0.73	0.86
	ME-01	6.85	181	50	24	5	120	2.32	1.53	102	0.42	0.52
	ME-02	7.27	413	101	15	4	313	2.76	0.79	140	0.68	0.53
	MO-01	6.93	219	58	28	5	143	1.98	0.82	91	0.37	0.65
	MO-02	6.90	202	52	21	5	140	2.49	1.63	117	0.57	0.96
	MS-04	6.23	97	35	30	3	34	2.14	1.13	94	0.30	0.65
	NE-03	6.78	159	37	27	5	104	3.01	3.43	124	0.40	0.70
	PS-02	6.68	116	35	11	5	74	3.13	4.33	149	0.80	0.50
	PS-03	6.73	130	39	17	4	83	1.76	0.72	102	0.52	0.82
	RA-01	7.14	302	60	16	5	239	3.06	1.41	108	0.51	0.94
	RO-01	6.45	108	47	19	5	51	3.56	1.19	128	0.68	0.43
	RO-04	6.91	196	52	10	5	150	3.51	0.75	152	1.41	0.85
	TE-01	7.18	316	38	21	4	271	2.39	1.20	96	0.32	0.84
	TE-03	7.15	291	41	16	5	246	2.19	0.95	107	0.53	0.79
	VA-01	6.69	150	43	26	5	98	2.87	1.30	91	0.40	1.14
	VS-02	6.94	200	45	22	3	152	2.93	1.18	111	0.42	0.70
	VS-04	6.63	119	31	23	4	76	3.17	1.31	93	0.25	0.68
	ZA-03	6.48	116	36	28	5	56	2.44	0.93	102	0.33	0.75
Acidic lakes[a]	ME-04	5.13	31	37	10	4	–3	5.2	2.6	182	1.26	0.69
	MO-06	4.96	38	38	28	5	–7	5.0	3.4	153	0.67	0.70
	NE-01	5.40	44	30	22	4	1	9.5	11.9	227	0.91	0.46
	SL-02	5.16	28	39	0.5	6	1	14.5	7.8	321	4.28	1.20
	ST-01	5.03	40	44	0.2	12	–3	14.3	11.7	454	6.19	0.48
	VS-15	5.33	33	33	6	4	0	7.6	9.2	235	1.37	0.26

[a] Non–acidic and acidic lakes had average ANC $\geq$ 20 and < 20 µeq L^{-1}, respectively, between 1992 and 2018.

[b] Average pH = –log(average H$^+$ activity).

Table SM-7. Slopes of linear regressions between concentrations and time for 31 Tatra Mountain lakes from 1992 to 2018. Significance: ***, $p<0.001$; **, $p<0.01$; and *, $p<0.05$. For full lake names and characteristics see Table SM-1; number of observations (n), sum of Ca^{2+} and Mg^{2+} concentrations (Ca+Mg), acid neutralizing capacity (ANC), total phosphorus (TP), chlorophyll-*a* (Chl-*a*), total organic nitrogen (TON), dissolved organic carbon (DOC), and dissolved silicon (Si). For τ-values and significance of Mann-Kendall test see Table SM-8.

	Lake	n	Ca+Mg	H⁺	SO₄²⁻	NO₃⁻	Cl⁻	ANC	TP	Chl-*a*	TON	DOC	Si
			---------------------- µeq L⁻¹ yr⁻¹ ----------------------						------- µg L⁻¹ yr⁻¹ -------			--- mg L⁻¹ yr⁻¹ ---	
Non-acidic lakes[a]	BA-01	27	0.01	−0.054**	−1.47***	−0.80***	0.02	1.97***	0.01	0.05***	3.04***	0.007*	0.010*
	BV-03	15	−0.95	−0.010*	−1.27**	−0.44**	−0.10*	2.36***	0.02	−0.01	1.53	0.013*	0.000
	BV-22	16	−1.24*	−0.025**	−1.72***	−0.66***	−0.10*	1.54***	−0.02	0.00	1.57	0.018***	0.001
	FU-01	27	1.83***	−0.081***	−1.21***	−0.55***	−0.10**	3.65***	0.03*	0.06***	4.07***	0.009**	0.003
	FU-04	17	1.02	−0.071***	−1.43***	−0.44*	−0.05*	3.10***	0.02	0.05	2.10	0.020***	0.005
	FU-07	24	−1.60***	−0.020***	−1.78***	−0.51***	−0.05**	0.98***	−0.07	0.01	2.82*	0.011	0.012
	GA-04	27	−1.07**	−0.111***	−1.85***	−1.08***	−0.09*	1.74***	0.04**	0.07	3.02***	0.017***	0.001
	GA-07	27	−1.38**	−0.007***	−1.81***	−0.56***	−0.08*	1.25***	0.00	0.09	2.12*	0.014*	0.002
	ME-01	27	0.28	−0.007**	−1.82***	−0.73***	−0.12**	2.68***	0.00	0.07**	2.07**	0.012*	−0.020**
	ME-02	27	3.03**	−0.003**	−1.69***	−0.44***	−0.02	5.10***	0.03	0.00	1.28	0.018**	0.011
	MO-01	27	−1.13*	−0.006**	−2.01***	−0.96***	−0.07*	1.87***	−0.02	−0.02	1.37	0.001	−0.006
	MO-02	26	−0.90	−0.007***	−2.00***	−0.58***	−0.07**	2.01***	0.02	0.04**	2.39**	0.013*	0.013**
	MS-04	15	−0.28	−0.141*	−1.11***	−0.83***	−0.08	2.09***	0.04	0.08*	3.23**	0.016**	0.005
	NE-03	27	0.71	−0.010***	−1.56***	−0.51***	−0.01	3.25***	0.00	0.10*	3.59***	0.011***	0.003
	PS-02	22	−1.06*	−0.010***	−1.85***	−0.66***	−0.12***	1.92***	0.00	0.02	2.68*	0.020*	−0.020**
	PS-03	23	−0.69	−0.008**	−1.56***	−0.46***	−0.11***	1.92***	0.00	0.01	1.37	0.014**	−0.002
	RA-01	27	0.34	−0.004**	−1.20***	−0.49***	−0.15***	3.00***	0.03	0.08**	2.40**	0.010	0.002
	RO-01	27	−0.54	−0.024***	−1.75***	−0.95***	0.00	2.25***	0.05*	0.04	3.51***	0.023***	−0.014
	RO-04	26	0.50	−0.005**	−1.82***	−0.45***	−0.07*	2.63***	0.03	0.02	1.84*	0.030**	0.003
	TE-01	21	1.07	−0.002*	−1.32***	−0.62***	−0.02	2.85***	−0.02	0.01	1.06	0.008*	0.006
	TE-03	16	0.46	−0.002**	−1.69***	−0.38**	−0.09**	2.85***	0.03**	0.02	2.26**	0.014***	0.003
	VA-01	17	−0.11	−0.040*	−1.71***	−0.75***	−0.07**	2.39***	−0.01	0.05	2.05*	0.015	0.009
	VS-02	17	−0.22	−0.004*	−1.80***	−0.84***	−0.03	2.03*	0.00	0.03	2.65*	0.010	0.005
	VS-04	27	0.43	−0.010***	−1.38***	−0.62***	−0.10**	2.24***	−0.04	0.01	1.31*	0.003	0.012
	ZA-03	16	−0.06	−0.033***	−1.24***	−0.71**	−0.07*	2.27***	0.00	0.04	3.33**	0.017***	0.007
Acidic lakes[a]	ME-04	26	−0.54***	−0.53***	−2.08***	−0.26*	0.06	0.66***	0.01	0.14	3.25**	0.041***	0.012**
	MO-06	26	−0.90***	−0.65***	−1.92***	−0.92**	−0.01	0.65***	0.07	0.12	3.51**	0.023***	0.010
	NE-01	27	−0.87**	−0.59***	−1.56***	−0.98***	−0.01	1.04***	0.37**	0.62	8.00**	0.032**	0.011**
	SL-02	27	−0.58***	−0.56***	−2.50***	−0.05**	0.04	0.92***	0.25	0.18	7.16***	0.088***	0.007
	ST-01	27	−1.15***	−0.77***	−2.68***	−0.02*	0.02	1.18***	−0.01	−0.16	5.28*	0.116**	−0.020
	VS-15	27	−0.59***	−0.55***	−2.15***	−0.19	0.08	0.86***	0.00	−0.18	3.34	0.023	0.002

[a]Non–acidic and acidic lakes had average ANC ≥ 20 and < 20 µeq L⁻¹, respectively, between 1992 and 2018 (Table SM-3).

Table SM-8. The τ-values of Mann-Kendall test for trends from Table SM-7 (except for Si). Significance: ***, $p<0.001$; **, $p<0.01$; and *, $p<0.05$.

	Lake	n	Ca+Mg	H⁺	SO₄²⁻	NO₃⁻	Cl⁻	ANC	TP	Chl-*a*	TON	DOC
Non-acidic lakes[a]	BA-01	27	0.09	−0.68***	−0.75***	−0.57***	−0.03	0.70***	0.06	0.55***	0.5***	0.46**
	BV-03	15	0.16	−0.37	−0.69***	−0.54**	−0.47*	0.52**	0.10	−0.36	0.05	0.40
	BV-22	16	−0.39*	−0.63***	−0.85***	−0.71***	−0.45*	0.80***	0.04	0.24	0.42	0.64**
	FU-01	27	0.57***	−0.77***	−0.81***	−0.75***	−0.44**	0.85***	0.20	0.56***	0.68***	0.42**
	FU-04	17	0.53**	−0.57**	−0.85***	−0.35	−0.24	0.72***	0.11	0.13	0.31	0.62**
	FU-07	24	−0.48**	−0.43**	−0.85***	−0.58***	−0.40**	0.56***	−0.30	0.13	0.35*	0.22
	GA-04	27	−0.36**	−0.64***	−0.83***	−0.66***	−0.30*	0.72***	0.45**	0.60***	0.54***	0.65***
	GA-07	27	−0.33*	−0.44**	−0.86***	−0.70***	−0.25	0.48***	0.03	0.20	0.37*	0.29*
	ME-01	27	0.04	−0.54***	−0.83***	−0.81***	−0.49***	0.77***	0.01	0.32*	0.33*	0.32*
	ME-02	27	0.49***	−0.42**	−0.63***	−0.51***	−0.16	0.72***	0.18	0.03	0.23	0.41**
	MO-01	27	0.16	−0.37*	−0.69***	−0.54**	−0.47*	0.52**	0.10	−0.36	0.05	0.40
	MO-02	26	−0.14	−0.41**	−0.84***	−0.77***	−0.30*	0.66***	0.05	0.41**	0.35*	0.47**
	MS-04	15	−0.05	−0.65***	−0.70***	−0.54**	−0.56**	0.77***	0.37	0.39	0.44*	0.68**
	NE-03	27	0.27	−0.56***	−0.86***	−0.59***	−0.19	0.84***	0.05	0.26	0.49***	0.43**
	PS-02	22	−0.16	−0.48**	−0.86***	−0.77***	−0.60***	0.77***	−0.01	−0.01	0.38*	0.29
	PS-03	23	−0.01	−0.42**	−0.80***	−0.69***	−0.57***	0.72***	0.03	0.23	0.20	0.37*
	RA-01	27	0.08	−0.41**	−0.66***	−0.57***	−0.41**	0.52***	0.19	0.39**	0.45**	0.27
	RO-01	27	−0.05	−0.59***	−0.73***	−0.70***	−0.01	0.79***	0.3*	0.30*	0.47***	0.59***
	RO-04	26	0.14	−0.36*	−0.74***	−0.68***	−0.37**	0.54***	0.23	0.23	0.37*	0.38*
	TE-01	21	0.17	−0.25	−0.72***	−0.72***	−0.09	0.63***	−0.05	0.06	0.32	0.46**
	TE-03	16	0.20	−0.36*	−0.92***	−0.63***	−0.43*	0.68***	0.17	−0.14	0.37	0.46*
	VA-01	17	0.15	−0.39*	−0.88***	−0.75***	−0.50**	0.77***	0.00	0.67***	0.34	0.32
	VS-02	17	0.05	−0.28	−0.78***	−0.65***	−0.30	0.41*	0.00	0.16	0.43*	0.35
	VS-04	27	0.16	−0.53***	−0.84***	−0.57***	−0.41**	0.68***	−0.15	0.07	0.26	0.3*
	ZA-03	16	0.10	−0.58**	−0.82***	−0.40*	−0.22	0.66***	−0.09	0.20	0.36	0.46*
Acidic lakes[a]	ME-04	26	−0.28*	−0.41**	−0.87***	−0.87***	−0.26	0.67***	−0.17	−0.17	0.24	0.03
	MO-06	26	−0.50***	−0.71***	−0.88***	−0.41**	0.00	0.66***	0.22	0.19	0.36*	0.51***
	NE-01	27	−0.44**	−0.66***	−0.76***	−0.56***	−0.08	0.56***	0.40**	0.31*	0.37*	0.47***
	SL-02	27	−0.50***	−0.73***	−0.89***	−0.21	0.08	0.59***	0.21	0.22	0.48***	0.45**
	ST-01	27	−0.73***	−0.59***	−0.84***	−0.21	0.01	0.66***	−0.06	−0.19	0.39**	0.30*
	VS-15	27	−0.65***	−0.73***	−0.87***	−0.18	−0.14	0.61***	−0.14	−0.24	0.03	0.19

[a]Non–acidic and acidic lakes had average ANC ≥ 20 and < 20 µeq L⁻¹, respectively, between 1992 and 2018 (Table SM-3).

Table SM-9. The τ-values of Mann-Kendall test for time series of concentrations of strong acid anions (SAAs), $Ca^{2+} + Mg^{2+}$, HCO_3^-, pH, total phosphorus (TP), chlorophyll a (Chl-a), dissolved organic carbon (DOC), and total organic nitrogen (TON) given in Figs. 1 and 2 for periods 1992–2018, 1992–2003, and 2004–2018. Significance: ***, $p<0.001$; **, $p<0.01$; and *, $p<0.05$. NA, non-acidic lakes; A, acidic lakes; ND, not determined.

	NA	A	NA	NA
	1992–2018	1992–2018	1992–2003	2004–2018
SAAs	−0.87***	−0.82***	ND	ND
$Ca^{2+} + Mg^{2+}$	ND	−0.71***	−0.55*	0.64**
HCO_3^-	0.72***	0.71***	ND	ND
pH	0.66***	0.76***	ND	ND
TP	0.02	0.28*	ND	ND
Chl-a	0.48***	0.04	ND	ND
DOC	0.64***	0.65***	ND	ND
TON	0.52***	0.49***	ND	ND

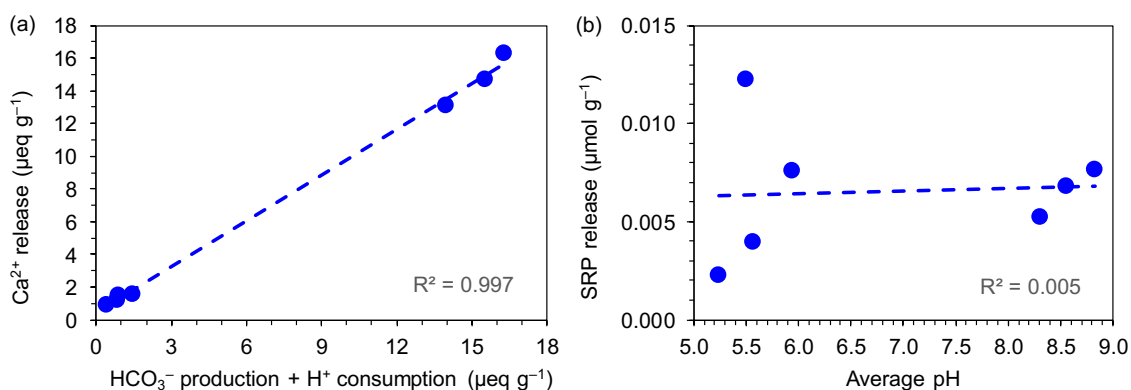**Part SM-4: Details to section: Results**
Extraction experiments

Fig. SM-3. Relationship between (a) dissolved carbonate (HCO_3^- production plus H^+ consumption) and Ca^{2+}, and (b) average final pH of extraction solution and soluble reactive phosphorus (SRP) extracted from the Tatra Mountain granodiorite rocks (samples G1, G2, G3, G6, G7, G8, and G11). All values are cumulative values for 15 consecutive extraction steps with diluted HNO_3 (original pH of 5.0). R^2 is coefficient of determination.

Additional references

Dougan WK, Wilson AL (1974) The absorptiometric determination of aluminium in water. A comparison of some chromogenic reagents and the development of an improved method. Analyst 99:413–430

Driscoll CT (1984) A procedure for the fractionation of aqueous aluminum in dilute acidic waters. Int J Environ An Ch 16:267–284

Fott J, Blažo M, Stuchlík E, Strunecký O (1999) Phytoplankton in three Tatra Mountain lakes in different acidification status. J Limnol 52:107–116

Golterman HL, Clymo RS (1969) Methods for chemical analysis of fresh waters. Blackwell, Oxford

Kopáček J, Hejzlar J (1993) Semi–micro determination of total phosphorus in fresh waters with perchloric acid digestion. Int J Environ An Ch 53:173–183

Kopáček J, Hejzlar J, Mosello R (2000) Estimation of organic acid anion concentrations and evaluation of charge balance in atmospherically acidified colored waters. Water Res 34:3598–3606

Procházková L (1960) Einfluss der Nitrate und Nitrite auf die Bestimmung des organischen Stickstoffs und Ammonimus im Wasser. Arch Hydrobiol 56:179–185